Science Advances
AAAS

advances.sciencemag.org/cgi/content/full/6/25/eaay5872/DC1

Supplementary Materials for

TET2 deficiency reprograms the germinal center B cell epigenome and silences genes linked to lymphomagenesis

Wojciech Rosikiewicz, Xiaowen Chen, Pilar M. Dominguez, Hussein Ghamlouch, Said Aoufouchi, Olivier A. Bernard, Ari Melnick*, Sheng Li*

*Corresponding author. Email: amm2014@med.cornell.edu (A.M.); sheng.li@jax.org (S.L.)

Published 17 June 2020, *Sci. Adv.* **6**, eaay5872 (2020)
DOI: 10.1126/sciadv.aay5872

This PDF file includes:

Supplementary Methods

RNA-seq

RNA-seq libraries for the *Vav-Cre* mouse model were generated using the TruSeq-stranded-mRNA sample kit (Illumina) following the Illumina single-end library preparation protocol. Single-end sequencing (SE50) was performed on an Illumina HiSeq2500. RNA-seq data were aligned to mm10 using STAR (*60*) and annotated to RefSeq reference annotation using the Subread package (*61*). RNA-seq libraries from *Aicda*$^{-/-}$ and *Aicda*$^{+/+}$ mice were prepared using the TruSeq RNA sample kit and sequenced on a HiSeq2000 sequencer, followed by the same computational analysis as described above. Differentially expressed genes (DEGs) were identified using the following strategy: 1) Genes with low expression, i.e., small numbers of reads over the analyzed samples, were removed prior to the analysis, as suggested by Ignatiadis et al.; (*62*). We adopted a threshold of at least 20 reads per gene mapped in all samples for this step; 2) Differential gene expression was computed using DESeq2 (*63*) for all remaining genes; 3) Using an independent filtering approach (*64*), the Benjamini and Hochberg correction for multiple hypothesis testing was applied to all genes with a positive differential expression covariate (i.e., absolute fold-change > 1.2), and all genes with FDR score less than 0.05 were considered as differentially expressed. For the purpose of the GSEA analysis, normalized expression levels were suabsequently exported as GCT files and postprocessed as described in the “GSEA” section below.

Microarray data analysis

Raw expression microarray readings from samples with DLBCL were processed using the Limma R package (*65*), including extraction from CEL files and normalization with RMA function. More specifically, we considered 7 samples with frameshift or stop codon gain mutations in the TET2 gene as TET2-mutated DLBCL, and 60 samples without any mutation of TET2 or CREBBP as a control ($TET2^{WT}$), as described previously (*14*). To calculate DEGs, microarray probe expression levels were transformed to log2 values and condensed using avereps. DEGs were called using lmFit and eBayes functions. FDR values lower than or equal to 0.05 were considered as significant, considering recomputed FDR scores for DEGs with a minimum of 1.5 FC. For the purpose of the GSEA analysis, normalized expression levels were subsequently exported as GCT files and postprocessed as described in the “GSEA” section below.

DNA methylation levels in human DLBCL samples with TET2 mutations, and their corresponding controls, were studied based on the results of Asmar et al. (*12*). More specifically, we utilized a precomputed list of 578 microarray probes hypermethylated in TET2-mutant samples (*12*). These probes were identified from global methylation profiling of the 12 DLBCL human patients with TET2 mutations and 18 TET2 wild-type cases, which was performed on the Infinium Human Methylation 450 Assay.

Hydroxymethylated DNA immunoprecipitation sequencing (hMeDIP-Seq)

Studies of 5hmC were conducted in *Vav-Cre/Tet2*$^{-/-}$ and *Vav-Cre/Tet2*$^{+/+}$ germinal center B-cells as described previously (*14*). More specifically, a total of 1.5 μg of gDNA was

sonicated with a Covaris S220. End repair, A-tailing, and ligation of the preannealed adapters were conducted before immunoprecipitation with the 5hmC antibody (1 µg/mL; Active Motif 39791). Ten percent of the volume was set aside as input before immunoprecipitation. To control the efficiency of the 5hmC pulldown, we used spike-ins (Diagenode AF-107-0040), and amplification of the libraries was performed using Kapa HiFi Hot Start Ready Mix (Kapa Biosystems, KK2601) for 12 cycles. Concentrations and quality of the final DNA libraries were measured by Qubit (Life Technologies) and an Agilent 2100 Bioanalyzer, respectively.

Sequencing of the libraries was performed in an Illumina HiSeq2500 multiplexing a single pulldown and a single input on each lane. Reads were trimmed using cutadapt 1.9.1 (*66*) and aligned by bowtie 2.0.5 (*67*). Unique reads were extracted using an in-house pipeline. MACS2 (*68*) peak caller "callpeak" function was used to detect broad peaks with the following parameters "–nomodel –extsize 200 -B –SPMR –broad –bw 200 –broad-cutoff 0.1". Subsequently, "bdgdiff" (from MACS2) was used to detect differential regions between *Vav-Cre/Tet2*$^{-/-}$ and *Vav-Cre/Tet2*$^{+/+}$ samples. Differentially hydroxymethylated regions (DHMRs) were annotated for introns, exons, promoters, and enhancers (defined as intergenic or intronic H3K27ac peaks from the study with the accession number GSE79640, excluding promoters). Promoter regions were defined as regions 2 kb upstream or downstream of the TSS of a gene. Enhancer regions were defined based on the presence of H3K27ac peaks in at least two samples from *Tet2*^{WT} and *Crebbp*^{WT} germinal center B-cells in mice, as described previously (*14*).

GSEA

All gene set enrichment analyses (GSEA), using GSEA software (*69, 70*), were conducted with settings based on a previously published leukemia study (*71*). The only exception was the change of the “permute” parameter to “gene_set” for the analysis of *Vav-Cre* mice germinal center B-cells, which is a consequence of dealing with sample sizes smaller than or equal to 7. As input files, we used the normalized gene expression levels from RNA-seq (*Vav-Cre/Tet2*$^{-/-}$ (n=4) samples and *Vav-Cre/Tet2*$^{+/+}$ (n=3) mouse GC B-cells) or microarray expression data (*TET2*^{MUT} (n=7) and *TET2*^{WT} (n=60) human DLBCL). GSEA was conducted against a database of gene sets, based on the publications of the Melnick and Straudt laboratories (*25, 72-74*), enlarged by the collection of gene signatures related with antigen processing and presentation and MHC genes, downloaded from GSKB database (*75*). In addition to that, the *Vav-Cre* mouse model was also tested against a collection of gene sets that are target genes of 13 transcription factors important for B-cell biology. These gene sets were obtained using RcisTarget (*76*). Specifically, we selected gene-motif rankings, which provided the rankings of all the 22,285 genes for each of 24,453 motifs using 500bp up- and down-stream of TSSs. The top 100 genes for each motif were considered as targets of all the transcription factors annotated to that motif. Because a transcription factor can be annotated to multiple motifs, different transcription factors have different numbers of targets depending on the number of motifs annotated to the transcription factor and overlap between the highly ranked genes for these motifs. All of these gene sets contain human gene IDs; therefore, in order to conduct the analysis, all genes in mice were converted to their orthologs in human based on cross-species annotation reference

orthology database, created at The Jackson Laboratory, downloaded (http://www.informatics.jax.org/downloads/reports/HOM_MouseHumanSequence.rpt) from Mouse Genome Database (MGD) (*77*).

In addition, enrichment of the above described gene sets was also tested using hypergeometric test for the following genes of interest:

- Figure 3A: 930 genes with hyper-DMCs in their promoters in *Tet2*$^{-/-}$ mouse GC B-cells (with Mm background)
- Figure 4E: 1,274 leading-edge genes of key transcription factor targets in mouse (with Mm background)
- Figure 6C, J: 3,111 genes related with aberrant *Aicda*$^{-/-}$ signature (with Mm background)
- Figure 6C, J: 1,949 genes with aberrant *Tet2*$^{-/-}$ signature (with Mm background)
- Figure 7B: 614 hyper-DMC genes in mouse (with Mm-Hs orthologs background)
- Figure 7B: 241 hyper-DMC genes in human (with Mm-Hs orthologs background)

Defining the number of successes in the sample as *k*, sample size as *s*, number of successes in the population as *M*, and population size as *N*, hypergeometric test was computed for all enriched gene sets. Enriched gene sets were defined as those in which the number of successes in the sample (*k*) was higher than the expected number of successes in the sample, with the assumption of random distribution, defined as $s * M/N$.

Finally, p-values for the enrichment of each set were corrected for multiple testing using the Benjamini–Hochberg correction.

SHM analysis

We amplified by PCR the genomic areas described previously as AID targets in the J_H4 (chr12:113,427,959-113,428,543) (*43*) and Sμ (chr12:113,425,655-113,426,278) (*42*) regions. The amplicons were pooled and cleaned up using the MinElute PCR Purification Kit (Qiagen). Sequencing libraries were constructed from the purified PCR product by using Illumina TruSeq DNA Sample Preparation Kit v2 (Illumina). Each sample was tagged with a unique index and sequenced on the Illumina MiSeq platform producing 2 × 300 bp paired-end reads. This experiment was conducted on GC B-cells ($B220^+Fas^+GL7^+$) from three *Vav-cre*/*Tet2*$^{+/+}$ and two *Vav-cre*/*Tet2*$^{-/-}$ replicates. PE 2 × 300 MiSeq reads were aligned to the *Mus musculus* GRCm38/mm10 genome using BWA-Mem (*78*), followed by variants calling with LoFreq program (*79*). Then, using bcftools (*80*), called variants were additionally filtered, excluding all known single-nucleotide polymorphisms (European Variation Archive accession GCA_000001635.6). Finally, in-house scripts were used to remove all variants with high variant allele frequency (>25%), and to narrow down the subsequent analysis to C-to-T (i.e., U) variants, located inside the WRC motif, which is a motif preferred by AID to deaminate cytosines to uracil (*44*). The per replicate allele frequency of the remaining variants was then used to compare pulled TET2 wild-type vs. TET2 deficient replicates.

As an orthogonal analysis, we have also used previously filtered reads for the analysis with the Immcantation pipeline (*81, 82*). More specifically, the

AssemblePairs.py, FilterSeq.py, CollapseSeq.py, and *SplitSeq.py* tools were used to construct clones of the J_H4 and Sμ regions represented by at least two pairs of paired-end reads. Next, clone sequences were aligned to the reference *Mus musculus* GRCm38/mm10 genome using BWA-MEM, and in-house scripts were used to identify C-to-T mutations at the AID-preferred motif, excluding alleles with high allele frequency (>25%) and known nucleotide polymorphisms. C-to-T mutations were then used to calculate the percentage of clones with at least one mutation, as well as the per-clone C-to-T mutation frequency normalized to 1 kb, computed as the number of mutations, divided by the clone length and multiplied by 1,000.

Supplementary Figures

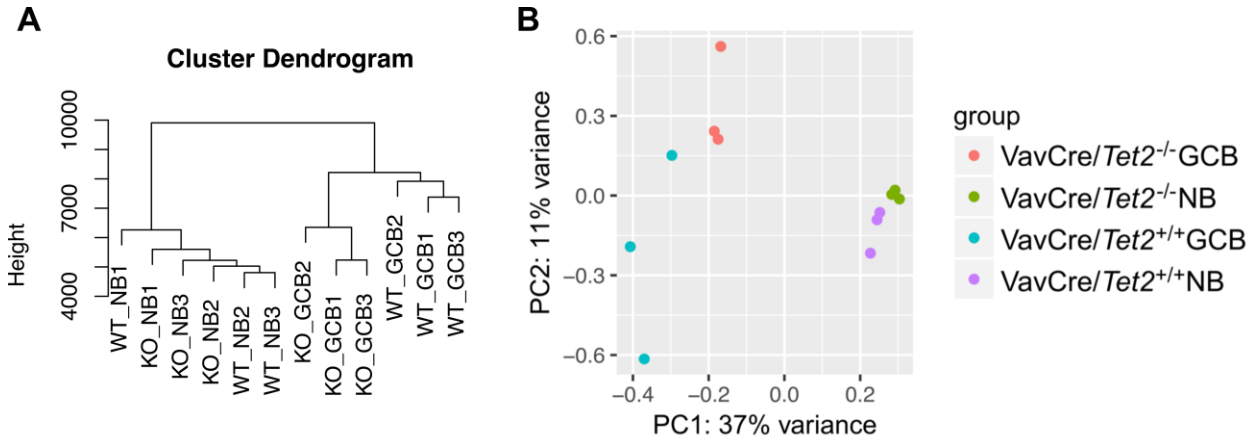

Supplementary Figure 1. *Tet2* deficiency leads to hypermethylation in germinal center B-cells and loss of hypomethylation during the NB-to-GCB transition. (A) Hierarchal clustering based on ERRBS data from three *Tet2*$^{-/-}$ and three *Tet2*$^{+/+}$ GCB samples as well as three *Tet2*$^{-/-}$ and three *Tet2*$^{+/+}$ naïve B-cell samples. NB – naïve B-cells, GCB – germinal center B-cells. (B) Principal component analysis based on ERRBS data from three *Tet2*$^{-/-}$ and three *Tet2*$^{+/+}$ GCB samples as well as three *Tet2*$^{-/-}$ and three *Tet2*$^{+/+}$ naïve B-cell samples.

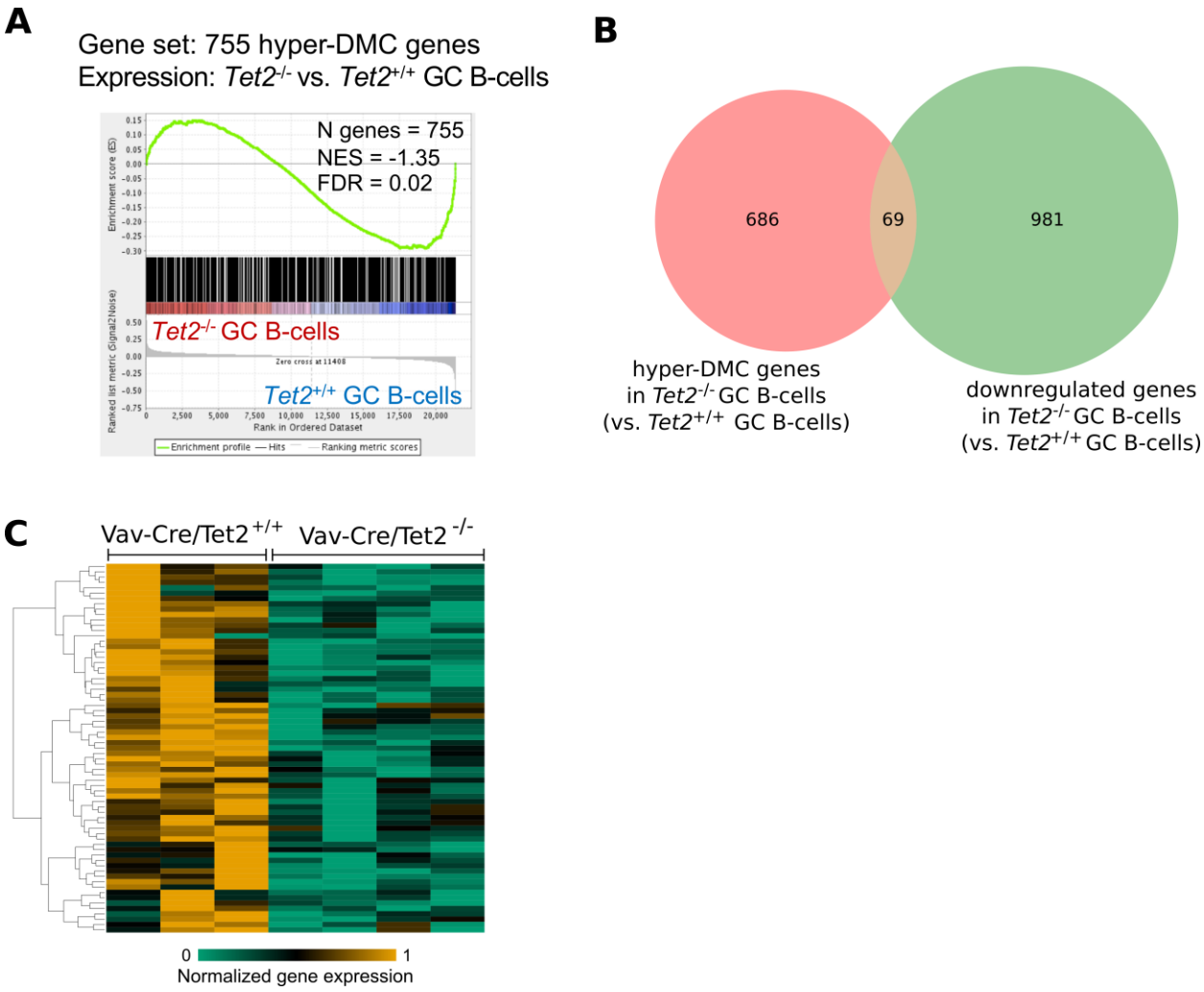

Supplementary Figure 2. Genes with hypermethylated promoters is significantly overlapping with the down-regulated genes. (A) Gene set enrichment analysis (GSEA) of 755 expressed genes with hyper-DMCs in promoters in *Tet2*-deficient germinal center (GC) B-cells. (B) Venn diagram of the overlap between genes with hyper-DMCs in their promoter regions and genes downregulated in TET2-deficient GC B-cells (in comparison with TET2 wild-type GC B-cells). (C). Heatmap of the expression of 69 downregulated genes with hyper-DMCs in their promoters.

A

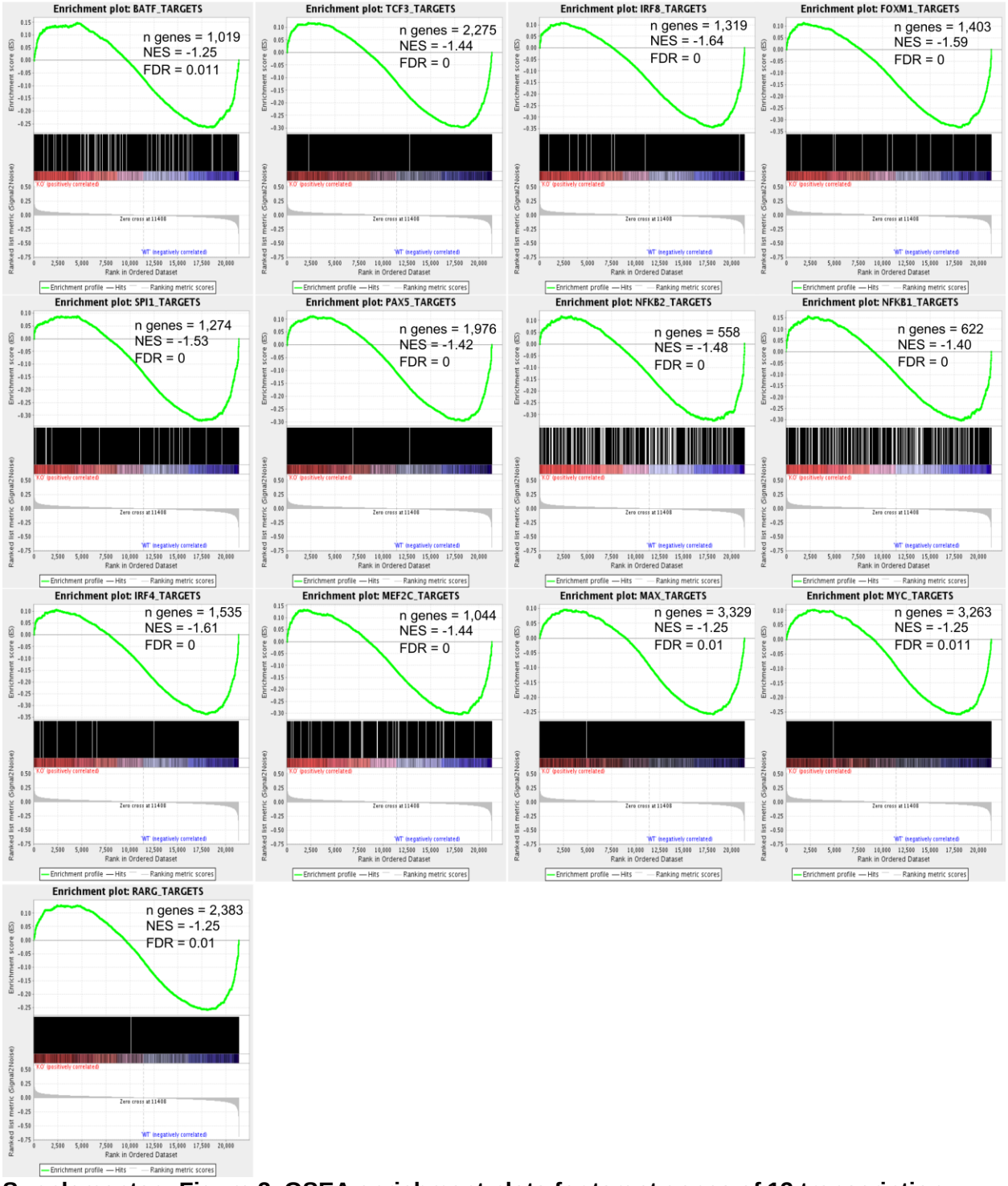

Supplementary Figure 3. GSEA enrichment plots for target genes of 13 transcription factors with hypermethylated binding sites in *Tet2*-deficient germinal center B-cells.

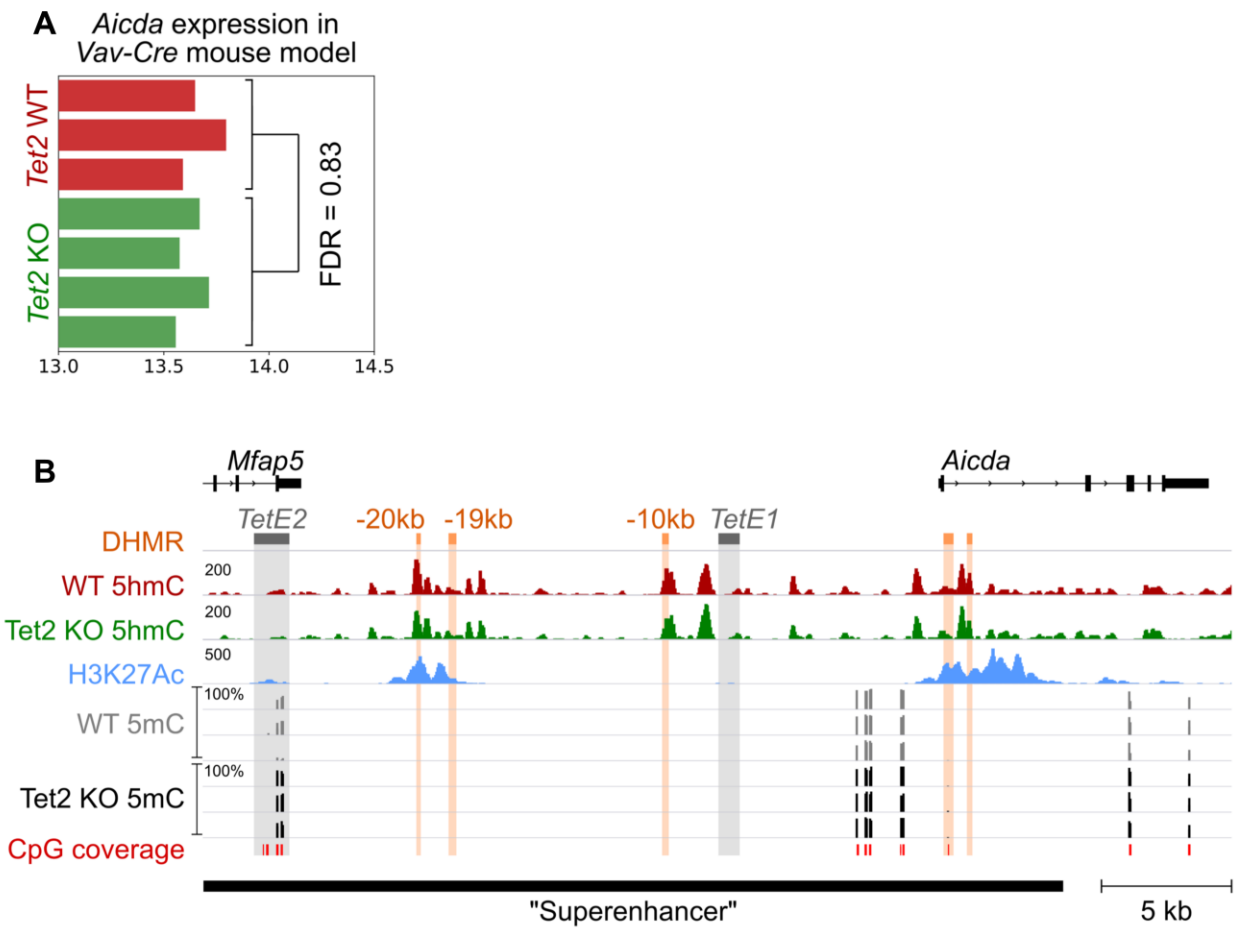

Supplementary Figure 4. Aicda expression are not affected by Tet2 deficiency. (A) Normalized expression level of *Aicda* in GC B-cells, *Vav-Cre* mouse model. (B) Genome browser view of the *Aicda* locus (mm10; chr6:122,525,514-122,565,126). TetE1, TetE2 and superenhancer regions were annotated based on Lio et al. 2019. FDR – false discovery rate, *Tet2* KO – *Vav-Cre/Tet2*$^{-/-}$, *Tet2* WT - *Vav-Cre/Tet2*$^{+/+}$. (C) Allele frequency of C-to-T mutations at WRC motif, where W = A or T, and R = G or A.

Supplementary Tables

Supplementary Table 1. Number of differentially methylated cytosines (DMCs).

Comparison	DMCs	hyper-DMCs	hypo-DMCs
Tet2 -/- GCBs[1] vs. Tet2 +/+ GCBs	10730	9043	1687
Tet2 -/- NBs[2] vs. Tet2 +/+ NBs	2091	1695	396
Tet2 -/- GCBs vs. Tet2 -/- NBs	14009	1168	12841
Tet2 +/+ GCBs vs. Tet2 +/+ NBs	22599	1449	21150

[1]GCBs - Germinal Center B-Cells
[2]NBs - Naïve B-Cells

Supplementary Table 2. Genomic distribution of hyper-DMCs.

Genomic regions						Hyper-DMCs	All CpGs	Hyper-DMC sites per 100 CpGs covered by BS-seq
Promoter	Intergenic	Exon	Intron	Enhancer	DHMR			
X						395	165474	0.2387
	X					2360	251789	0.9373
		X				732	94809	0.7721
			X			2243	190377	1.1782
X					X	13	255	5.0980
	X				X	46	413	11.1380
		X			X	77	742	10.3774
			X		X	60	604	9.9338
	X			X		384	13660	2.8111
		X		X		163	2383	6.8401
			X	X		629	10242	6.1414
X			X			830	285289	0.2909
X		X				745	440327	0.1692
X			X		X	63	562	11.2100
X		X			X	80	804	9.9502
	X			X	X	75	348	21.5517
		X		X	X	38	265	14.3396
			X	X	X	110	680	16.1765

Supplementary Table 3. Leading edge hypermethylated and repressed genes.

GENE	Rank in gene list	Rank metric score	Running enrichment score
TOX2	21353	-0.584854662	9.74E-05
MCF2L	21347	-0.463383079	-0.01800285
IGKV14-130	21346	-0.441906333	-0.032536075
NPR2	21344	-0.429306298	-0.04634718
TRP73	21293	-0.268854588	-0.057384577
SMOC1	21291	-0.267973185	-0.065768205
CACNG6	21289	-0.263072014	-0.07412419
PLXND1	21265	-0.228224173	-0.08125855
SNX18	21249	-0.221290231	-0.08768829
H2-Q7	21235	-0.212922469	-0.09399765
FAH	21223	-0.206816643	-0.100141644
NACC2	21198	-0.192208678	-0.10546311
MICU1	21185	-0.184027463	-0.11090891
C030005K06RIK	21173	-0.175820142	-0.11614667
TMEM154	21166	-0.173160121	-0.12136972
RAI2	21151	-0.168731362	-0.12612101
GAS7	21146	-0.166631445	-0.13121882
NDRG1	21128	-0.159864157	-0.13561974
TLR6	21127	-0.159760937	-0.14063361
NRXN2	21101	-0.153602943	-0.1444307
DMPK	21072	-0.147759452	-0.14788905
AI480526	21066	-0.146057531	-0.15228057
VANGL1	21047	-0.143082604	-0.15598767
PTMS	21033	-0.141352698	-0.15984417
DPP4	20983	-0.132433698	-0.16189894
CDKL4	20926	-0.124176182	-0.16333418
GM16793	20871	-0.117960617	-0.16460752
RAPGEFL1	20869	-0.117644995	-0.16825862
ASS1	20846	-0.116039224	-0.17088044
SLC11A1	20839	-0.115383193	-0.17422856
DYRK4	20834	-0.114946991	-0.17765321
ZBTB38	20832	-0.11487025	-0.18120977
DNASE1L3	20831	-0.114779428	-0.18481249
GATM	20817	-0.113268547	-0.18778132
CHD5	20799	-0.111776352	-0.19050859
MICAL3	20796	-0.111441553	-0.19391719
ECHDC3	20760	-0.107851408	-0.19571342
YPEL2	20734	-0.104893431	-0.19788246
DGKH	20732	-0.104715623	-0.20112371
SPAG8	20700	-0.102270745	-0.20290317
HOPXOS	20686	-0.101396918	-0.20547968
TUBG2	20663	-0.09950643	-0.2075919
LHPP	20661	-0.099422783	-0.21066423
ADAM19	20651	-0.098428465	-0.21334557
BCAS1	20583	-0.094522804	-0.21318035
ZFHX2	20582	-0.094522722	-0.21614489
FCRLA	20555	-0.09279713	-0.21784736
PSAP	20532	-0.091631517	-0.21968988
RINL	20509	-0.089960478	-0.22149584

ZBTB12	20504	-0.089519717	-0.22412314
GM26698	20497	-0.089249313	-0.22663952
GM13496	20465	-0.087843858	-0.2279339
GM19705	20436	-0.086374342	-0.22932981
GM4779	20421	-0.085995786	-0.23135921
RHBDF1	20419	-0.08589828	-0.23400779
FCGR4	20415	-0.085815541	-0.23655622
NFKBIA	20402	-0.085091271	-0.23866518
LDLRAP1	20399	-0.084950656	-0.24123684
STOML1	20380	-0.084137335	-0.24302743
GML	20377	-0.084052563	-0.24556917
RARG	20365	-0.083204009	-0.24767138
TNFAIP8	20353	-0.082745247	-0.24974698
C5AR2	20337	-0.082242332	-0.25161403
METTL21A	20256	-0.0797133	-0.25031012
CRB3	20225	-0.078657478	-0.25135395
DTX1	20199	-0.077538379	-0.25260738
P2RX4	20134	-0.074861079	-0.2519326
VAMP1	20125	-0.074530028	-0.25389215
HK1	20046	-0.072275884	-0.25244343
MAP7D1	20035	-0.071961254	-0.25422484
MIB2	20021	-0.071293429	-0.25585073
MTUS1	19989	-0.070260994	-0.25658196
TMEM8B	19981	-0.070180945	-0.25844577
HINT2	19975	-0.070114486	-0.26040417
KREMEN2	19918	-0.068477824	-0.2598849
KCNJ10	19914	-0.06837938	-0.26188695
FCAMR	19838	-0.06645669	-0.26039097
RAP1GAP	19828	-0.066033453	-0.26203838
AFMID	19817	-0.065839089	-0.263624
MTSS1L	19814	-0.065799899	-0.26559186
VIM	19797	-0.065371089	-0.2668789
SFXN3	19782	-0.064985052	-0.26824957
CPLX2	19762	-0.0645997	-0.26936543
RUSC2	19758	-0.064483464	-0.27124587
CDK5R1	19740	-0.064209007	-0.2724431
LPO	19715	-0.063493088	-0.2732919
PGF	19705	-0.063168027	-0.27484637
PECAM1	19662	-0.06226043	-0.2747888
CDHR5	19644	-0.061873972	-0.27591628
SLC16A8	19640	-0.061808653	-0.27771124
FAM169B	19595	-0.060805101	-0.27751395
FAM184A	19552	-0.059994489	-0.27738225
APITD1	19546	-0.059825718	-0.27902117
MUC20	19523	-0.059477776	-0.2798296
RAB26	19521	-0.059455194	-0.28164646
CLEC4A1	19509	-0.059324421	-0.28297722
PCDHGA12	19485	-0.058898229	-0.2837214
WNT5B	19481	-0.058841489	-0.285423
ST3GAL1	19476	-0.058722496	-0.2870743
COX14	19440	-0.057845701	-0.28721708
ZFP516	19402	-0.057126872	-0.2872353
GM15232	19369	-0.056602329	-0.28747365
TAPBP	19346	-0.056126185	-0.28818098

PGPEP1L	19322	-0.055617798	-0.28882483
GM11841	19304	-0.055311952	-0.289744
RP23-45G16.6	19194	-0.053450566	-0.28618777
STON2	19115	-0.052101858	-0.2840779
FUT1	19109	-0.051937982	-0.2854693
GM8731	19010	-0.05037383	-0.28234118
LBH	19003	-0.050269704	-0.28362983
MIR6913	18926	-0.049166895	-0.28151733
HOXA6	18878	-0.04862234	-0.2807779
NFKBIB	18863	-0.048332985	-0.2816233
SPON1	18836	-0.047904238	-0.2818771
MAMSTR	18832	-0.047789779	-0.2832339
TTLL1	18785	-0.047169682	-0.28249985
OST4	18744	-0.046585731	-0.2820376
1110059E24RIK	18730	-0.046362579	-0.28286764
ACY1	18728	-0.046325877	-0.28427318
ANXA2	18722	-0.04626878	-0.28548342
STIM2	18712	-0.046112936	-0.28649768
SPNS2	18589	-0.044775456	-0.28202188
HERPUD1	18568	-0.044529885	-0.28245538
HIC1	18476	-0.043176979	-0.2794347
GATSL3	18464	-0.043070816	-0.28025493
KATNAL1	18461	-0.043031473	-0.28150868
GM10717	18429	-0.042702787	-0.28135353
IKBKE	18421	-0.042584281	-0.28235304
4930578M01RIK	18403	-0.042362787	-0.2828634
IRF8	18402	-0.042347107	-0.28419206
H2-KE6	18394	-0.042245369	-0.28518042
MAST1	18391	-0.042230926	-0.28640828
DNASE2A	18382	-0.04213557	-0.28734446
IRAK2	18373	-0.042067543	-0.28827763
SH2D3C	18359	-0.041892257	-0.28896597
IFI30	18344	-0.041740302	-0.28960028
FAM83G	18332	-0.041608602	-0.29037544
LPHN1	18293	-0.041027293	-0.28983584
PLA1A	18281	-0.040897395	-0.29058865
ARAP1	18250	-0.040598176	-0.29041508
CDC42SE1	18235	-0.04045533	-0.2910088

Supplementary Table 4. **Pathways enriched in genes with promoter hypermethylation in TET2-deficient GC B-cells.**

Pathway	log2FC	p-value	FDR
c3.Crebbp.down 500	1.768418205	4.73E-08	1.24E-05
CTCF NB all	0.270910987	2.18E-06	0.000189461
P300 ly1 enhancer	0.847696041	2.12E-06	0.000189461
CTCF NB enhancer	0.299304033	5.58E-06	0.000291299
CTCF CB all	0.248254259	5.26E-06	0.000291299
Myc ChIP PET 2plus	0.454352228	2.23E-05	0.000972162
PU.1 CB enhancer	0.331931125	3.00E-05	0.001120399
CTCF CB enhancer	0.255758339	4.11E-05	0.001340258
PU.1 NB enhancer	0.302307089	4.71E-05	0.001366217
PU.1 CB all	0.275676649	6.46E-05	0.00168653
Pan B U133plus	2.106113616	9.02E-05	0.002139363
GCB bivalentProm genes	0.530293254	0.000144261	0.002940357
Ly1 BCL6RD2mut upreg	0.600700442	0.000146455	0.002940357
Blimp Bcell repressed	2.269612348	0.000200439	0.003736762
CTCF ly1 all	0.151113601	0.000289409	0.005035724
denovobivGenes	0.697409078	0.000393515	0.006419206
Resting blood B cell GNF	1.954110522	0.000458432	0.0064858
BACH2 target ChIPseq	0.330058684	0.000445472	0.0064858
LZvsDZ Teater CC Up vs CB	0.989504429	0.000472146	0.0064858
B cell down anergy	3.854574849	0.000667956	0.008716828
PU.1 NB all	0.214763871	0.000760488	0.00882042
P300 ly1 all	0.214763871	0.000760488	0.00882042
mouse.shCrebbp.r2.down p.500	1.181256474	0.000780733	0.00882042
mouse shCrebbp.r2.down 545	0.939463747	0.000811073	0.00882042
mouse.shCrebbp.r2.0 p.1000 down	0.906489618	0.000945635	0.009872429
ly1.promoter.BCL6-SMRT.all.451	0.870694514	0.001987191	0.01861418
ly1.enhancer.INTRONIC.BCL6-SMRT.DRE.807	0.643427185	0.001967223	0.01861418
CTCF ly1 enhancer	0.146706201	0.001996924	0.01861418
c1.Crebbp.down 500	0.989504429	0.002288318	0.020594861
KLF2 induced	1.392760579	0.003118313	0.02712932
NB GCB Progression All Genes RPKM plus5	0.877294925	0.003235286	0.027233106
KEGG ANTIGEN PROCESSING AND PRESENTATION	1.813932864	0.003443266	0.027233106
GO BP MM ANTIGEN PROCESSING AND PRESENTATION OF EXOGENOUS PEPTIDE ANTIGEN VIA MHC CLASS II	3.176502944	0.003405307	0.027233106
CD40 upregulated Burkitt lymphoma	1.494678904	0.004510702	0.033769875
Leucine starve up	1.323051607	0.004528527	0.033769875
Glutamine Glucose starve both down	0.776572337	0.004846681	0.035138441

HSC e-ERY down Ebert cell 11	0.684649847	0.005944982	0.041936221
Bcell down Ebert cell 11	0.891100725	0.006135627	0.042142067
Germinal center Bcell DLBCL	1.818950939	0.006510986	0.043573519
CTCF ly1 prom	0.220668882	0.006830508	0.044569062
Myeloma TACI high bone marrow plasma cell gene	1.369148022	0.007973505	0.050758166
c3.Crebbp.up 500	1.143079942	0.008375526	0.052047908
ly1.enhancer.INTRONIC.DISTAL.BCL6-SMRT.DRE.1275	0.447222098	0.009372912	0.056722976
CTCF CB prom	0.311814847	0.009779823	0.056722976
GO CC MM MHC CLASS II PROTEIN COMPLEX	3.591540443	0.009751216	0.056722976
MD901.loss.5.enhancer.g	0.450015867	0.010746819	0.060976515
ABC gt GCB LC	2.591540443	0.011815143	0.065611751
KMT2D DOWN DEGS MOUSE	0.506052544	0.013606336	0.073984454
Resting dendritic cell GNF	1.306138224	0.015411406	0.082089324
NB GCB Progression All Genes RPKM minus2	0.413347826	0.016289689	0.082602139
IKZF1 CB enhancer	0.657967805	0.017090098	0.082602139
CTCF NB prom	0.287759695	0.016802069	0.082602139
c1.Crebbp.down 397	0.778772025	0.016056195	0.082602139
GO ANTIGEN PROCESSING AND PRESENTATION	0.923161934	0.016571147	0.082602139
MD901.loss.25.enhancer.g	0.262069586	0.017871231	0.084807115
Myc ChIP PET Expr Down	0.784185521	0.02121569	0.098880268

Supplementary Table 5. Leading edge genes enriched for hyper-DMCs genes impacting key pathways in B-cell biology.

GENE SYMBOL	RANK IN GENE LIST	RANK METRIC SCORE	RUNNING ES
TAPBP	19346	-0.056126185	-0.425361
ZFP516	19402	-0.057126872	-0.42144212
ST3GAL1	19476	-0.058722496	-0.41819063
APITD1	19546	-0.059825718	-0.41462457
CDK5R1	19740	-0.064209007	-0.4164097
SFXN3	19782	-0.064985052	-0.41093418
VIM	19797	-0.065371089	-0.40414062
FCAMR	19838	-0.06645669	-0.39845008
DTX1	20199	-0.077538379	-0.40659523
CRB3	20225	-0.078657478	-0.39880568
C5AR2	20337	-0.082242332	-0.3946653
RARG	20365	-0.083204009	-0.3864517
LDLRAP1	20399	-0.084950656	-0.37832204
NFKBIA	20402	-0.085091271	-0.3687136
PSAP	20532	-0.091631517	-0.3643519
FCRLA	20555	-0.09279713	-0.35480848
ZFHX2	20582	-0.094522722	-0.345257
BCAS1	20583	-0.094522804	-0.33447874
ADAM19	20651	-0.098428465	-0.32641652
LHPP	20661	-0.099422783	-0.31550416
YPEL2	20734	-0.104893431	-0.3069407
MICAL3	20796	-0.111441553	-0.2971115
CHD5	20799	-0.111776352	-0.2844602
DNASE1L3	20831	-0.114779428	-0.27283484
DPP4	20983	-0.132433698	-0.26485863
PTMS	21033	-0.141352698	-0.2510525
NDRG1	21128	-0.159864157	-0.23725887
NACC2	21198	-0.192208678	-0.21859741
H2-Q7	21235	-0.212922469	-0.1960169
SNX18	21249	-0.221290231	-0.17139693
PLXND1	21265	-0.228224173	-0.14608069
TRP73	21293	-0.268854588	-0.11669763
MCF2L	21347	-0.463383079	-0.06635964
TOX2	21353	-0.584854662	9.45E-05

Supplementary Table 6. Hyper-DMCs in TET2-deficient GC B-cells are significantly overrepresented with binding sites of transcription factors essential for B-cells development.

Motif Name	Consensus	P-value	q-value (Benjamini)	% of Target Sequences with Motif
ZNF711(Zf)/SHSY5Y-ZNF711-ChIP-Seq(GSE20673)/Homer	AGGCCTAG	1.00E-10	0	35.94%
E2A(bHLH),near_PU.1/Bcell-PU.1-ChIP-Seq(GSE21512)/Homer	NVCACCTGBN	1.00E-10	0	28.41%
ZFX(Zf)/mES-Zfx-ChIP-Seq(GSE11431)/Homer	AGGCCTRG	1.00E-10	0	25.21%
Elk4(ETS)/Hela-Elk4-ChIP-Seq(GSE31477)/Homer	NRYTTCCGGY	1.00E-08	0	20.37%
HEB(bHLH)/mES-Heb-ChIP-Seq(GSE53233)/Homer	VCAGCTGBNN	1.00E-07	0	34.81%
Ptf1a(bHLH)/Panc1-Ptf1a-ChIP-Seq(GSE47459)/Homer	ACAGCTGTTN	1.00E-07	0	43.89%
Slug(Zf)/Mesoderm-Snai2-ChIP-Seq(GSE61475)/Homer	SNGCACCTGCHS	1.00E-06	0	12.18%
NFkB-p50,p52(RHD)/Monocyte-p50-ChIP-Chip(Schreiber_et_al.)/Homer	GGGGGAATCCCC	1.00E-06	0	3.06%
PU.1:IRF8(ETS:IRF)/pDC-Irf8-ChIP-Seq(GSE66899)/Homer	GGAAGTGAAAST	1.00E-05	0.0005	3.76%
E2A(bHLH)/proBcell-E2A-ChIP-Seq(GSE21978)/Homer	DNRCAGCTGY	1.00E-04	0.0007	27.19%
Elk1(ETS)/Hela-Elk1-ChIP-Seq(GSE31477)/Homer	HACTTCCGGY	1.00E-04	0.0007	18.72%
EBF2(EBF)/BrownAdipose-EBF2-ChIP-Seq(GSE97114)/Homer	NABTCCCWDGGGAVH	1.00E-04	0.0015	15.85%
Ascl1(bHLH)/NeuralTubes-Ascl1-ChIP-Seq(GSE55840)/Homer	NNVVCAGCTGBN	1.00E-04	0.0028	27.66%
Mef2c(MADS)/GM12878-Mef2c-ChIP-Seq(GSE32465)/Homer	DCYAAAAATAGM	1.00E-03	0.0045	3.81%
Max(bHLH)/K562-Max-ChIP-Seq(GSE31477)/Homer	RCCACGTGGYYN	1.00E-03	0.0048	10.25%
FOXA1(Forkhead)/MCF7-FOXA1-ChIP-Seq(GSE26831)/Homer	WAAGTAAACA	1.00E-03	0.0066	8.65%
AP-1(bZIP)/ThioMac-PU.1-ChIP-Seq(GSE21512)/Homer	VTGACTCATC	1.00E-03	0.0066	8.75%
ZNF322(Zf)/HEK293-ZNF322.GFP-ChIP-Seq(GSE58341)/Homer	GAGCCTGGTACTGWGCCTGR	1.00E-03	0.0066	5.79%
IRF4(IRF)/GM12878-IRF4-ChIP-Seq(GSE32465)/Homer	ACTGAAACCA	1.00E-03	0.007	5.60%
Oct2(POU,Homeobox)/Bcell-Oct2-ChIP-Seq(GSE21512)/Homer	ATATGCAAAT	1.00E-03	0.0071	2.96%
AP-2gamma(AP2)/MCF7-TFAP2C-ChIP-Seq(GSE21234)/Homer	SCCTSAGGSCAW	1.00E-03	0.0091	20.56%
Tcf7(HMG)/GM12878-TCF7-ChIP-Seq(Encode)/Homer	CTTTGATGTGSB	1.00E-03	0.0091	4.23%
Tbet(T-box)/CD8-Tbet-ChIP-	AGGTGTGAAM	1.00E-03	0.0091	13.08%

Seq(GSE33802)/Homer				
EBF1(EBF)/Near-E2A-ChIP-Seq(GSE21512)/Homer	GTCCCCWGGGGA	1.00E-03	0.0091	19.19%
Jun-AP1(bZIP)/K562-cJun-ChIP-Seq(GSE31477)/Homer	GATGASTCATCN	1.00E-03	0.0091	3.48%
ETV4(ETS)/HepG2-ETV4-ChIP-Seq(ENCODE)/Homer	ACCGGAAGTG	1.00E-03	0.012	26.76%
RARg(NR)/ES-RARg-ChIP-Seq(GSE30538)/Homer	AGGTCAAGGTCA	1.00E-02	0.0243	1.18%
ETV1(ETS)/GIST48-ETV1-ChIP-Seq(GSE22441)/Homer	AACCGGAAGT	1.00E-02	0.0266	28.79%
EBF(EBF)/proBcell-EBF-ChIP-Seq(GSE21978)/Homer	DGTCCCYRGGGA	1.00E-02	0.0266	4.09%
PAX5(Paired,Homeobox)/GM12878-PAX5-ChIP-Seq(GSE32465)/Homer	GCAGCCAAGCRTGACH	1.00E-02	0.0266	6.49%
Mef2d(MADS)/Retina-Mef2d-ChIP-Seq(GSE61391)/Homer	GCTATTTTTAGC	1.00E-02	0.0322	1.93%
JunB(bZIP)/DendriticCells-Junb-ChIP-Seq(GSE36099)/Homer	RATGASTCAT	1.00E-02	0.0327	6.30%
Atf3(bZIP)/GBM-ATF3-ChIP-Seq(GSE33912)/Homer	DATGASTCATHN	1.00E-02	0.0376	7.43%
IRF3(IRF)/BMDM-Irf3-ChIP-Seq(GSE67343)/Homer	AGTTTCAKTTTC	1.00E-02	0.0376	4.19%
BATF(bZIP)/Th17-BATF-ChIP-Seq(GSE39756)/Homer	DATGASTCAT	1.00E-02	0.0431	7.15%
ZEB1(Zf)/PDAC-ZEB1-ChIP-Seq(GSE64557)/Homer	VCAGGTRDRY	1.00E-02	0.0448	30.95%
Fosl2(bZIP)/3T3L1-Fosl2-ChIP-Seq(GSE56872)/Homer	NATGASTCABNN	1.00E-02	0.0448	4.28%
ZBTB18(Zf)/HEK293-ZBTB18.GFP-ChIP-Seq(GSE58341)/Homer	AACATCTGGA	1.00E-02	0.0454	7.76%
n-Myc(bHLH)/mES-nMyc-ChIP-Seq(GSE11431)/Homer	VRCCACGTGG	1.00E-02	0.0512	10.96%
ZEB2(Zf)/SNU398-ZEB2-ChIP-Seq(GSE103048)/Homer	GNMCAGGTGTGC	1.00E-02	0.0512	18.44%
RUNX(Runt)/HPC7-Runx1-ChIP-Seq(GSE22178)/Homer	SAAACCACAG	1.00E-02	0.0512	10.54%
p63(p53)/Keratinocyte-p63-ChIP-Seq(GSE17611)/Homer	NNDRCATGYCYNRRCATGYH	1.00E-02	0.0512	5.32%
Fra2(bZIP)/Striatum-Fra2-ChIP-Seq(GSE43429)/Homer	GGATGACTCATC	1.00E-02	0.0512	5.60%
FOXA1(Forkhead)/LNCAP-FOXA1-ChIP-Seq(GSE27824)/Homer	WAAGTAAACA	1.00E-02	0.0566	10.16%
FOXM1(Forkhead)/MCF7-FOXM1-ChIP-Seq(GSE72977)/Homer	TRTTTACTTW	1.00E-02	0.0609	8.89%
c-Myc(bHLH)/mES-cMyc-ChIP-Seq(GSE11431)/Homer	VVCCACGTGG	1.00E-02	0.0629	7.53%
Oct4(POU,Homeobox)/mES-Oct4-ChIP-Seq(GSE11431)/Homer	ATTTGCATAW	1.00E-02	0.0838	3.90%

Supplementary Table 7. Pathways enriched by B-cell biology key TF targets with repressed gene expression.

Pathway	log2FC	p-value	FDR
CTCF ly1 all	0.7549	4.34E-151	1.54E-148
CTCF ly1 enhancer	0.8333	8.31E-136	1.48E-133
CTCF CB all	0.8722	1.60E-112	1.89E-110
CTCF CB enhancer	0.9505	3.60E-101	3.20E-99
CTCF NB all	0.8371	1.20E-92	8.50E-91
CTCF NB enhancer	0.9266	4.18E-85	2.48E-83
PU.1 NB enhancer	0.9279	9.69E-70	4.92E-68
PU.1 NB all	0.8009	3.29E-69	1.30E-67
P300 ly1 all	0.8009	3.29E-69	1.30E-67
PU.1 CB enhancer	0.9659	4.77E-65	1.69E-63
PU.1 CB all	0.8392	2.66E-64	8.57E-63
GC termDiff Genes	1.4581	8.68E-41	2.57E-39
GCB bivalentProm genes	1.3182	2.76E-40	7.53E-39
PU.1 target ChIPseq Ebert Cell 11	0.9985	1.81E-38	4.58E-37
Ly1 BCL6RD2mut upreg	1.3234	1.46E-33	3.45E-32
c1.Crebbp.down 397	2.2103	7.82E-33	1.73E-31
NB GCB Progression All Genes RPKM minus2.to.plus2	0.8197	8.51E-33	1.78E-31
EZH2 target ChIP	1.2779	3.63E-28	7.15E-27
Ly1 siBCL6 48h upreg	1.3511	4.24E-28	7.92E-27
mouse shCrebbp.r2.down 545	1.8676	2.63E-26	4.66E-25
CTCF ly1 prom	0.6655	1.05E-24	1.77E-23
GMP up Ebert cell 11	1.5453	1.31E-23	2.11E-22
denovobivGenes	1.3953	5.06E-23	7.81E-22
Tcell down Ebert cell 11	1.4248	3.93E-21	5.81E-20
BACH2 target ChIPseq	0.6544	1.61E-19	2.28E-18
Myc ChIP PET 2plus	0.7641	6.99E-19	9.54E-18
KMT2D DOWN DEGS MOUSE	1.2561	3.14E-18	4.13E-17
c2.Crebbp.down 295	1.9516	3.77E-18	4.62E-17
c2.Crebbp.down 500	1.9516	3.77E-18	4.62E-17
HSC up Ebert cell 11	1.2636	2.57E-17	3.04E-16
LZvsDZ Teater CC Up vs CB	1.6479	7.79E-17	8.92E-16
Lymph node DLBCL	2.1726	7.43E-16	8.24E-15
Monocyte 4x U133plus	1.9143	1.65E-15	1.77E-14
c2.Ep300.down 468	1.5897	3.76E-14	3.92E-13
GCB BCL6SMRT Distal Enhancer	1.4240	5.27E-14	5.34E-13
NB GCB Progression All Genes RPKM minus2	0.9663	7.14E-13	7.05E-12
mouse.shCrebbp.r2.0 p.1000 down	1.4176	1.25E-12	1.20E-11
GC T helper up2x Chtanova	1.4459	1.91E-12	1.78E-11
Resting monocyte GNF	1.9202	5.85E-12	5.33E-11
c1.Ep300.down 692	1.2137	7.86E-12	6.98E-11
CNS PNS Node1663	1.7045	8.92E-12	7.72E-11
ly1.enhancer.INTRONIC.DISTAL.BCL6-SMRT.DRE.1275	0.9066	1.75E-11	1.48E-10
CTCF CB prom	0.6723	1.84E-11	1.52E-10
HSC e-ERY down Ebert cell 11	1.1908	3.20E-11	2.59E-10
Monocyte 8x U133plus	2.1260	2.44E-10	1.93E-09
NB GCB Progression All Genes RPKM plus2	0.8559	3.39E-10	2.62E-09
HIF1alpha 1.5x Up	1.8376	1.57E-09	1.19E-08

CTCF NB prom	0.5993	2.54E-09	1.88E-08
CNS Node1661	2.1926	2.65E-09	1.92E-08
NFkB Targets	1.8678	3.53E-09	2.51E-08
NB GCB Progression All Genes RPKM enhancer loss minus3 minus4	1.2227	4.00E-09	2.78E-08
MD901.loss.25.enhancer.g	0.5342	7.16E-09	4.89E-08
ERY down Ebert cell 11	0.6899	7.82E-09	5.24E-08
P300 ly1 enhancer	0.8580	8.26E-09	5.43E-08
CD8 T effectorDn memoryIm NaiveUp	2.9516	8.54E-09	5.51E-08
NFkB all OCILy3 Ly10	2.3063	9.17E-09	5.82E-08
c1.Crebbp.down 500	1.4078	1.00E-08	6.23E-08
BCL6 target ChIPseq	0.5000	1.62E-08	9.89E-08
ly1.promoter.BCL6.all.3140	0.4995	1.67E-08	1.00E-07
Dendritic cell CD123pos blood	1.3693	2.18E-08	1.27E-07
EZH2 mut down 347 Ash FL	1.2968	2.18E-08	1.27E-07
IRF3 target gene	1.6677	2.63E-08	1.51E-07
c3.Crebbp.down 500	1.5593	3.34E-08	1.88E-07
NFkB Targets Young.Lab	1.5783	3.98E-08	2.21E-07
HRAS overexpression 2x up	1.7030	4.63E-08	2.53E-07
MD901.loss.5.enhancer.g	0.7749	5.55E-08	2.99E-07
NB GCB Progression All Genes RPKM plus5	1.2644	6.09E-08	3.23E-07
ly1.enhancer.INTRONIC.BCL6-SMRT.DRE.807	0.8951	7.17E-08	3.74E-07
GC T helper up4x Chtanova	1.6722	7.36E-08	3.79E-07
GCB.promoter.BCL6.all.5541	0.3416	8.76E-08	4.44E-07
GCB.promoter.BCL6-BCOR.all.5451	0.3375	1.70E-07	8.48E-07
ly1.enhancer.DISTAL.BCL6-SMRT.DRE.553	1.0771	1.73E-07	8.52E-07
MEIS1 target ChIPseq Ebert Cell 11	1.0013	2.92E-07	1.42E-06
GC B cell BLlow DLBCLhigh	2.4456	3.02E-07	1.45E-06
Thymic SP CD4+Tcell gt Blood CD4+Tcell	2.0460	4.28E-07	2.02E-06
GC B cell U133Plus	1.3004	5.15E-07	2.41E-06
IL6 Ly10 Up all	2.4821	6.33E-07	2.92E-06
PU.1 NB prom	0.4148	6.97E-07	3.17E-06
c3.Crebbp.up 500	1.6364	1.05E-06	4.74E-06
Enhancer loss.ATAC.reads CREBBP.KD	0.8921	1.64E-06	7.27E-06
PU.1 CB prom	0.4462	1.72E-06	7.52E-06
161 ANTIGEN or MHC combined	1.5540	1.80E-06	7.81E-06
Resting dendritic cell GNF	1.9066	1.84E-06	7.88E-06
B cell up anergy	2.9796	2.35E-06	9.93E-06
NB GCB Progression All Genes RPKM enhancer gain plus3 plus4	1.1732	3.13E-06	1.29E-05
NB GCB Progression All Genes RPKM plus10	1.1732	3.13E-06	1.29E-05
Thymic SP CD4+Tcell gt Thymic DP Tcell	1.6748	3.42E-06	1.40E-05
Quiescence heme cluster1	1.5023	3.47E-06	1.40E-05
IKZF1 CB enhancer	1.0284	3.53E-06	1.41E-05
ly1.promoter.BCL6-SMRT.all.451	1.0143	3.62E-06	1.43E-05
Myeloid Node1536	2.8971	4.01E-06	1.55E-05
NB GCB Progression All Genes RPKM minus5	1.1964	3.98E-06	1.55E-05
Myc ChIP PET Expr Down	1.2062	4.68E-06	1.77E-05
mouse.shCrebbp.r2.down p.500	1.2731	4.65E-06	1.77E-05
Bcell down Ebert cell 11	1.1548	5.67E-06	2.12E-05
IL10 OCILy3 Up	1.5767	6.06E-06	2.24E-05
ABC gt GCB Affy	2.8191	6.56E-06	2.40E-05
Serum response Fb up	1.3381	8.08E-06	2.93E-05
NFkB bothOCILy3andLy10	2.2786	8.80E-06	3.16E-05

Dendritic cell CD16pos blood	2.2411	1.16E-05	4.12E-05
HRAS overexpression 4x up	1.8447	1.28E-05	4.51E-05
Enhancer gain.ATAC.reads CREBBP.KD	1.4207	1.44E-05	5.01E-05
Tcell cytokine induced PMBC Bcell induced	2.4821	1.64E-05	5.64E-05
IFN PMBC 2x Up	1.5064	2.11E-05	7.22E-05
CREBBP.mouse.ChIPseq.LOSS.25.enhancer	0.6374	2.15E-05	7.27E-05
ARID1A mut up 141 Ash FL	1.4821	2.72E-05	9.12E-05
Bcell up Ebert cell 11	0.5840	3.31E-05	0.0001097
ly1.promoter.BCL6-BCOR.all.2142	0.4502	3.71E-05	0.0001211
Tcell up Ebert cell 11	0.4804	3.72E-05	0.0001211
Tcell cytokine induced IL2 IL7 IL15only	2.7045	4.70E-05	0.0001517
IKZF1 CB all	0.6137	4.83E-05	0.0001543
Tcell PIrep CalciumDefPtup4x Feske Fig6	2.0346	5.05E-05	0.0001601
HSC e-ERY up Ebert cell 11	0.4773	9.72E-05	0.0003053
IKAROS target ChIPseq Young Ebert Cell 11	0.6312	0.000134	0.0004174
MCL gt SLL DLBCL	2.7451	0.0001398	0.0004315
Quiescence heme all	1.0156	0.0001541	0.0004715
PMBL HL high	1.7694	0.0001584	0.0004805
ly1.promoter.BCL6.SMRT.BCOR.341	0.9598	0.0001616	0.0004862
Tcell PIind CsAdown4x	1.7451	0.0001873	0.0005588
NB GCB Progression All Genes RPKM minus10	1.5890	0.0001897	0.0005613
Tcell PIind4x CsAindependent	2.6520	0.0002124	0.000623
GCB.promoter.BCL6.SMRT.BCOR.1306	0.5144	0.0002175	0.0006278
GCB.promoter.BCL6-SMRT.all.1306	0.5144	0.0002175	0.0006278
IRF4 myeloma induced Lymphochip	1.3422	0.0002409	0.0006896
GCB.promoter.BCL6-BCOR.only.4145	0.2779	0.0002626	0.0007458
p53 targets	1.4232	0.0002733	0.0007699
IL6 Ly10 Up group1	2.3509	0.0002782	0.0007778
CD40 upregulated Burkitt lymphoma	1.4662	0.0003013	0.0008291
STAT3high ABC DLBCL subgroup	1.4662	0.0003013	0.0008291
Intron gain.ATAC.reads CREBBP.KD	1.6520	0.0003527	0.0009632
Regulatory Tcell FOXP3+ 3x gt CD4+Tcell	2.2895	0.0003727	0.00101
IFN PMBC 4x Up	1.6297	0.0004094	0.0010982
Intron loss.ATAC.reads CREBBP.KD	0.9918	0.0004114	0.0010982
ABC gt GCB LC	2.8040	0.0004171	0.001105
Regulatory T cell McHugh Herman concensus	2.4821	0.000444	0.0011676
Blood CD4+Tcell gt thymic SP CD4+Tcell	1.8040	0.0004499	0.0011744
TAL1 target ChIPseq Ebert Cell 11	1.6936	0.0004756	0.0012324
I-ERY down Ebert cell 11	0.3584	0.0005232	0.0013418
GO ANTIGEN PROCESSING AND PRESENTATION	1.0596	0.0005254	0.0013418
Plasma cell gt mature Bcell	2.0227	0.0005703	0.0014462
GO REGULATION OF ANTIGEN PROCESSING AND PRESENTATION	2.4041	0.0006164	0.0015518
mouse shCrebbp.r2.up 328	0.9702	0.0006526	0.0016315
JAK IL10 Ly10 Up	1.9796	0.0007072	0.0017557
IL6 Ly10 Up group2	3.0671	0.0007269	0.0017921
Dendritic cell CD123pos tonsil	2.3301	0.0008363	0.0020476
Myeloma MF subgroup down	1.9378	0.0008694	0.0020995
LSC 42 Dick NatMed 11	1.9378	0.0008694	0.0020995
Tcell cytokine induced IL2 IL7 IL15 IL4	2.5816	0.0009536	0.0022567
Distal loss.ATAC.reads CREBBP.KD	0.7941	0.0009482	0.0022567
GO BP MM ANTIGEN PROCESSING AND PRESENTATION OF EXOGENOUS PEPTIDE	2.5816	0.0009536	0.0022567

ANTIGEN VIA MHC CLASS II			
Tcell PIind4x Feske Fig6	1.3666	0.0009622	0.002262
STAT3 up OCILy10	1.8971	0.00106	0.0024757
HIF1alpha 2x Up	1.6341	0.0011895	0.00276
Distal gain.ATAC.reads CREBBP.KD	1.3925	0.0012177	0.0028071
Myeloma MS subgroup up	1.8576	0.0012826	0.0029376
IRF4 myeloma induced all	0.8498	0.0013297	0.0030259
CLL mutated gt CLL unmutated	2.4821	0.0013604	0.0030762
Cell cycle Cho	0.6716	0.0015869	0.0035654
Pancreas Node1629	2.7451	0.0019801	0.0043933
Regulatory Tcell FOXP3+ 4x gt CD4+Tcell	2.7451	0.0019801	0.0043933
c1.Crebbp.up 198	1.1602	0.0020647	0.0045525
TGFbeta up epithelial large	1.7451	0.00218	0.0047771
BCL6 repressed	2.3015	0.0025367	0.0055248
GO ANTIGEN PROCESSING AND PRESENTATION OF PEPTIDE ANTIGEN	0.9881	0.0026692	0.0057779
ly1.promoter.BCL6-SMRT.only.93	1.3301	0.0026925	0.0057929
CD8 T effectorUp memoryIm NaiveDn	2.0082	0.0029575	0.0063248
Tcell PIind4x Feske Fig4	1.3122	0.002993	0.0063623
Myeloma LB subgroup up	1.7870	0.0034357	0.0071627
Tcell cytokine repressed	1.7870	0.0034357	0.0071627
LPC LSC 52 Alizadeh JAMA 10	1.7870	0.0034357	0.0071627
NK up Ebert cell 11	1.2284	0.0034502	0.0071627
Tcell cytokine induced PBMC Bcell nochange	1.9516	0.0036534	0.0075404
KLF2 induced	1.1602	0.0038162	0.0078309
ly1.promoter.BCL6.alone.906	0.4840	0.0039351	0.0080285
GCB.DLBCL 1085 intersectSignature Matt	0.4300	0.0046849	0.0095037
Tcell cytokine induced PMBConly Iinduced	1.7045	0.0048055	0.0096929
ly1.promoter.BCL6-BCOR.only.1783	0.3359	0.0048696	0.0097668
Blimp Bcell repressed	1.4296	0.0055759	0.0111205
GO POSITIVE REGULATION OF ANTIGEN PROCESSING AND PRESENTATION	2.3666	0.0058372	0.0115765
E2F3 overexpression 2x up	1.0800	0.0062888	0.0124029
Myeloma TACI high bone marrow plasma cell gene	1.2411	0.0064114	0.0125749
Myc ChIP PET 3plus	0.6520	0.0069656	0.0135868
HRAS overexpression 2x down	1.4821	0.0070208	0.013599
Tcell PIrep4x Feske Fig6	1.3790	0.0070485	0.013599
NFkB OCILy10 only	2.2597	0.0077906	0.0149496
PAX5 repressed	1.3544	0.007888	0.0150551
Tcell PIind CalciumDefPtdown4x Feske Fig6	1.2597	0.0083453	0.0158427
CREBBP mut down 278 Ash FL	0.7451	0.0092974	0.0175562
GC B cell BL equal DLBCL	0.8474	0.0095358	0.0179112
Resting blood NK cell GNF	1.5169	0.0099944	0.0186738
T NK Node1604	2.1602	0.0101289	0.0188259
CD4 T U133plus	3.4821	0.0102466	0.0189456
GO ANTIGEN PROCESSING AND PRESENTATION OF PEPTIDE OR POLYSACCHARIDE ANTIGEN VIA MHC CLASS II	1.1342	0.0110841	0.0203878
HSC down Ebert cell 11	1.3666	0.0113576	0.0207833
Endothelial precursor GNF	1.6076	0.0123193	0.0224275
CREBBP mut up 334 Ash FL	0.6621	0.0125636	0.0227555
NFkB OCILy3 only	2.4821	0.0135619	0.024439
Resting panT cell CD4+CD8+ GNF	1.2146	0.0146165	0.0262063
c1.Ep300.up 381	0.6265	0.0151785	0.0270772

KRAS Up	1.1926	0.0160563	0.0285
HSC 120 Dick NatMed 11	0.9796	0.0183206	0.0322481
EZH2 mut up 124 Ash FL	0.9346	0.0183496	0.0322481
GO ANTIGEN PROCESSING AND PRESENTATION VIA MHC CLASS IB	2.3301	0.0185256	0.032397
IRF4 myeloma induced direct	1.4821	0.0186254	0.0324118
Resting blood B cell GNF	1.1495	0.0192434	0.033324
ERY up Ebert cell 11	0.3266	0.0198708	0.0342433
KRAS Down	1.2895	0.0228546	0.039195
GC T helper down Kim	1.8191	0.0237942	0.0405564
Myeloma MF subgroup up	1.4041	0.0238769	0.0405564
BreastCa 70gene Good	2.1926	0.0243607	0.0406012
CD8 T effectorDn memoryDn NaiveUp	2.1926	0.0243607	0.0406012
GO REGULATION OF ANTIGEN PROCESSING AND PRESENTATION OF PEPTIDE ANTIGEN	2.1926	0.0243607	0.0406012
GO BP MM INFLAMMATORY RESPONSE TO ANTIGENIC STIMULUS	2.1926	0.0243607	0.0406012
GC B cell BLhigh DLBCLlow	1.5310	0.0269256	0.0446663
Tcell PIrep CsAup4x	1.7451	0.0283741	0.0468502
Myeloma CD-2 subgroup up	1.3301	0.0300362	0.0491376
Myeloma LB subgroup down	1.3301	0.0300362	0.0491376
CD40 downregulated Burkitt lymphoma	1.1129	0.03036	0.0494394
B cell down anergy	2.7451	0.0315164	0.0510883
CLL unmutated gt CLL mutated	1.6748	0.0334415	0.0537671
Splenic marginal zone Bcell gt GC Bcell	1.2945	0.0334719	0.0537671
Notch T-ALL down Palomero	1.9516	0.038637	0.0617844
Dendritic cell BDCA3pos blood	1.0447	0.0388286	0.0618124
Tcell PIind CalciumDefPtdown4x Feske Fig4	1.1195	0.0405099	0.0642009
IKZF1 CB prom	0.3580	0.041375	0.0652806
DC TLR4 TLR8 synergy	1.5435	0.0450561	0.069811
OCAB up	2.4821	0.0454263	0.069811
PMBLhigh HLlow	2.4821	0.0454263	0.069811
GO ANTIGEN PROCESSING AND PRESENTATION OF ENDOGENOUS ANTIGEN	1.5435	0.0450561	0.069811
GO BP MM POSITIVE REGULATION OF MHC CLASS II BIOSYNTHETIC PROCESS	2.4821	0.0454263	0.069811
GO BP MM POSITIVE REGULATION OF DENDRITIC CELL ANTIGEN PROCESSING AND PRESENTATION	2.4821	0.0454263	0.069811
Pan B U133plus	0.9585	0.0523841	0.0801567
KLF2 repressed	0.8344	0.0534464	0.0810832
GO ANTIGEN PROCESSING AND PRESENTATION OF PEPTIDE ANTIGEN VIA MHC CLASS I	0.8344	0.0534464	0.0810832
BreastCa 70gene Bad	1.2597	0.0550174	0.0827592
Follicular lymphoma Immune Response1	1.2597	0.0550174	0.0827592
Follicular dendritic cell	4.0671	0.059661	0.0857475
GO BP MM POSITIVE REGULATION OF TOLERANCE INDUCTION TO SELF ANTIGEN	4.0671	0.059661	0.0857475
GO MF MM ENDOGENOUS LIPID ANTIGEN BINDING	4.0671	0.059661	0.0857475
GO BP MM NEGATIVE REGULATION OF CHRONIC INFLAMMATORY RESPONSE TO ANTIGENIC STIMULUS	4.0671	0.059661	0.0857475

GO BP MM REGULATION OF TOLERANCE INDUCTION TO SELF ANTIGEN	4.0671	0.059661	0.0857475
GO BP MM ANTIGEN TRANSCYTOSIS BY M CELLS IN MUCOSAL-ASSOCIATED LYMPHOID TISSUE	4.0671	0.059661	0.0857475
GO BP MM NEGATIVE REGULATION OF ACUTE INFLAMMATORY RESPONSE TO ANTIGENIC STIMULUS	4.0671	0.059661	0.0857475
GO BP MM MHC CLASS II BIOSYNTHETIC PROCESS	4.0671	0.059661	0.0857475
GO BP MM REGULATION OF MHC CLASS I BIOSYNTHETIC PROCESS	4.0671	0.059661	0.0857475
GO BP MM NEGATIVE REGULATION PEPTIDE OR POLYSACCHARIDE ANTIGEN VIA MHC CLASS II	4.0671	0.059661	0.0857475
GO BP MM NEGATIVE REGULATION OF DENDRITIC CELL ANTIGEN PROCESSING AND PRESENTATION	4.0671	0.059661	0.0857475
Normal mesenchymal-2 Node1615	2.2597	0.0611236	0.0874954
Notch T-ALL up Weng	1.0671	0.0645597	0.092043
GC T helper up Chtanova and Kim	1.6520	0.0662957	0.0937648
Splenic Marginal zone Bcell gt naive and GC Bcell	1.6520	0.0662957	0.0937648

Supplementary Table 8. **TET2-deficient and AID-deficient GC B-cells enriched pathways.**

Pathway	AID(enriched FDR)	TET2(enriched FDR)
CTCF_ly1_all	1.47E-71	1.09E-20
shCrebbp.down_1028	6.24E-60	1.42E-19
P300_ly1_all	4.13E-30	4.19E-18
PU.1_NB_all	4.13E-30	4.19E-18
PU.1_CB_all	1.55E-26	1.64E-17
PU.1_CB_enhancer	5.85E-19	2.03E-17
CTCF_NB_all	2.06E-45	9.67E-17
CTCF_CB_all	1.73E-46	5.67E-16
CTCF_ly1_prom	5.70E-40	1.16E-14
BACH2_target_ChIPseq	2.30E-30	1.16E-14
PU.1_NB_enhancer	1.57E-18	1.16E-14
CTCF_NB_prom	1.44E-25	2.92E-12
CTCF_ly1_enhancer	6.32E-40	1.53E-11
MD901.loss.25.enhancer.g	6.28E-27	1.57E-11
shCrebbp.down_500	8.25E-19	4.18E-11
CTCF_CB_prom	4.98E-22	2.13E-10
PU.1_target_ChIPseq_Ebert_Cell_11	4.63E-13	3.89E-10
mouse.shCrebbp.r2.0_p.1000_down	2.66E-19	4.06E-10
Myc_ChIP_PET_2plus	1.61E-15	1.17E-09
CTCF_NB_enhancer	3.36E-24	3.12E-09
GC_termDiff_Genes	4.73E-23	7.68E-09
CTCF_CB_enhancer	3.36E-24	1.79E-08
MD901.loss.5.enhancer.g	3.63E-15	3.53E-08
shEp300.down_636	2.02E-28	9.80E-08
Myc_Targets	1.16E-17	1.08E-07
mouse_shCrebbp.r2.down_545	5.23E-18	2.12E-06
GCB.promoter.BCL6.all.5541	3.28E-30	2.32E-06
GMP_up_Ebert_cell_11	1.54E-06	2.32E-06
CREBBP.mouse.ChIPseq.LOSS.25.prom	1.74E-13	2.55E-06
GCB.promoter.BCL6-BCOR.all.5451	1.89E-29	3.00E-06
PU.1_NB_prom	5.30E-13	3.45E-06
MD901.loss.25.prom.g	2.06E-28	5.24E-06
PU.1_CB_prom	4.60E-11	5.24E-06
CREBBP.mouse.ChIPseq.LOSS.25.enhancer	6.22E-10	5.73E-06
I-ERY_down_Ebert_cell_11	1.66E-14	7.30E-06
P300_ly1_enhancer	2.42E-08	9.77E-06
Tcell_up_Ebert_cell_11	1.70E-10	1.55E-05
NB_GCB_Progression_All_Genes_RPKM_minus2.to.plus2	1.95E-15	2.76E-05
mouse.shCrebbp.r2.down_p.500	4.71E-10	3.35E-05
GCB.promoter.BCL6-BCOR.only.4145	1.28E-21	5.12E-05
Tcell_PIrep_CalciumDefPtup4x_Feske_Fig6	0.022046302	5.12E-05
IKZF1_CB_all	1.74E-06	7.59E-05
LZvsDZ_Teater_CC_Up_vs_CB	0.000685044	8.07E-05
Myc_ChIP_PET_Expr_Down	0.016484676	0.0001021
Hematopoietic_Node1658	0.022692274	0.0001021
BCL6_target_ChIPseq	1.45E-12	0.00013544
ly1.promoter.BCL6.all.3140	1.50E-12	0.00013586
MD901.loss.5.prom.g	1.78E-14	0.00014713
HSC_e-ERY_up_Ebert_cell_11	3.30E-25	0.00017353

Proliferation_DLBCL	2.41E-13	0.00025815
GO_ANTIGEN_PROCESSING_AND_PRESENTATION_OF_PEPTIDE_ANTIGEN_VIA_MHC_CLASS_I	0.009607981	0.00044057
GO_ANTIGEN_PROCESSING_AND_PRESENTATION	0.025625032	0.00052699
Myeloma_MF_subgroup_up	0.000148304	0.00067283
EZH2_mut_up_124_Ash_FL	0.291367293	0.00067283
HSC_e-ERY_down_Ebert_cell_11	0.000311769	0.00067593
IKZF1_CB_enhancer	0.000311769	0.00083786
c3.Crebbp.down_500	0.016290061	0.00089506
NB_GCB_Progression_All_Genes_RPKM_plus5	0.016458732	0.00100242
KMT2D_DOWN_DEGS_MOUSE	0.022692274	0.00105515
Blimp_proliferation_repressed	0.001323949	0.00116316
Proliferation_Node1606	2.21E-07	0.00119259
IFN_PMBC_2x_Up	0.000614	0.00132924
GO_ANTIGEN_PROCESSING_AND_PRESENTATION_OF_EXOGENOUS_PEPTIDE_ANTIGEN_VIA_MHC_CLASS_I	0.026831918	0.00165751
GO_BP_MM_ANTIGEN_PROCESSING_AND_PRESENTATION_OF_ENDOGENOUS_PEPTIDE_ANTIGEN_VIA_MHC_CLASS_I	0.069690287	0.00165751
ly1.enhancer.INTRONIC.BCL6-SMRT.DRE.807	0.03212458	0.0017467
XBP1_target_all	7.95E-06	0.003282
GO_ANTIGEN_PROCESSING_AND_PRESENTATION_OF_PEPTIDE_ANTIGEN	0.031620541	0.00330613
HSC_down_Ebert_cell_11	0.004666612	0.00377134
KEGG_ANTIGEN_PROCESSING_AND_PRESENTATION	0.036058108	0.00421296
GCB_BCL6SMRT_Distal_Enhancer	0.001737317	0.00454579
ly1.promoter.BCL6-BCOR.all.2142	2.76E-10	0.00481873
NK_down_Ebert_cell_11	2.84E-07	0.00493817
ERY_down_Ebert_cell_11	0.001299393	0.00494627
P300_ly1_prom	4.80E-12	0.00508039
ly1.enhancer.INTRONIC.DISTAL.BCL6-SMRT.DRE.1275	0.003630785	0.00533782
Glutamine_Glucose_starve_both_down	1.08E-08	0.00561781
c1.Ep300.up_381	1.37E-07	0.00561781
Enhancer_loss.ATAC.reads_CREBBP.KD	7.40E-05	0.00563123
Leucine_starve_up	0.000460671	0.00605525
XBP1_target_secretory	0.000704979	0.00629955
Tcell_PIrep4x_Feske_Fig6	0.01044834	0.00691309
c1.Crebbp.down_397	0.022692274	0.00735433
Tcell_down_Ebert_cell_11	8.52E-05	0.00846249
Resting_monocyte_GNF	0.053423268	0.00846249
Myc_ChIP_PET_Expr_Up	1.63E-09	0.00922095
NFkB_Targets_Young.Lab	0.096109442	0.00973728
IL10_OCILy3_Up	0.006838889	0.01040554
NB_GCB_Progression_All_Genes_RPKM_plus2	0.01116681	0.012804
Lymph_node_DLBCL	0.022120433	0.0134695
ly1.promoter.BCL6-BCOR.only.1783	1.48E-07	0.01549229
B_cell_up_anergy	0.368395699	0.01671149
Distal_loss.ATAC.reads_CREBBP.KD	0.001754392	0.01671652
GO_CC_MM_MHC_CLASS_I_PEPTIDE_LOADING_COMPLEX	0.291367293	0.01671652

Blimp_Bcell_repressed	0.368829672	0.01716499
HIF1alpha_1.5x_Up	0.01066673	0.01823231
Glutamine_starve_down	1.31E-06	0.01897542
c1.Crebbp.down_500	0.101760436	0.0198151
NFkB_Targets	0.03566405	0.02068972
161_ANTIGEN_or_MHC_combined	0.16275601	0.02112893
IRF3_target_gene	0.058146353	0.02136608
MEIS1_target_ChIPseq_Ebert_Cell_11	0.002458238	0.02195175
GCB_bivalentProm_genes	1.62E-11	0.02195653
Ly1_BCL6RD2mut_upreg	0.000106674	0.02507041
Leucine_starve_down	0.000685044	0.02669243
Pan_B_U133plus	0.046235535	0.02669243
Myc_ChIP_PET_3plus	0.013421636	0.0282007
Myeloma_HY_subgroup_down	0.093116426	0.0282007
I-ERY_up_Ebert_cell_11	4.81E-07	0.03012104
IL6_Ly10_Up_all	0.000311769	0.03027326
HRAS_overexpression_2x_up	0.210008426	0.03070377
c3.Crebbp.up_500	0.029905822	0.0317874
Dendritic_cell_CD123pos_blood	0.086441999	0.03491076
ly1.promoter.BCL6.alone.906	0.006185949	0.03564387
denovobivGenes	1.66E-06	0.03580179
Intron_loss.ATAC.reads_CREBBP.KD	0.003526566	0.03580179
T_cell	0.007489716	0.03580179
GO_BP_MM_ANTIGEN_PROCESSING_AND_PRESENTATION_OF_EXOGENOUS_PEPTIDE_ANTIGEN_VIA_MHC_CLASS_II	0.03212458	0.03580179
CD40_upregulated_Burkitt_lymphoma	0.341466877	0.03796932
Resting_blood_NK_cell_GNF	0.136421423	0.0424607
c2.Crebbp.down_295	0.003526566	0.04327385
c2.Crebbp.down_500	0.003526566	0.04327385
T_NK_Node1604	0.01066673	0.04397001
GCB.promoter.BCL6-SMRT.all.1306	1.03E-06	0.05846945
GCB.promoter.BCL6.SMRT.BCOR.1306	1.03E-06	0.05846945
Notch_T-ALL_up_Sharma	0.020784672	0.06036437
IKAROS_target_ChIPseq_Young_Ebert_Cell_11	4.64E-05	0.0616581
ly1.promoter.BCL6-SMRT.all.451	0.001306059	0.06515989
Bcell_down_Ebert_cell_11	0.000103692	0.06590389
GO_BP_MM_ANTIGEN_PROCESSING_AND_PRESENTATION_OF_EXOGENOUS_PEPTIDE_ANTIGEN_VIA_MHC_CLASS_I	0.435247175	0.06590389
NB_GCB_Progression_All_Genes_RPKM_minus2	0.004665623	0.0665098
JAK_IL10_Ly10_Up	0.008502547	0.0665098
GO_MF_MM_MHC_CLASS_I_PROTEIN_BINDING	0.154019129	0.0665098
GO_ANTIGEN_PROCESSING_AND_PRESENTATION_VIA_MHC_CLASS_IB	NA	0.0665098
Endothelial_precursor_GNF	0.174868274	0.07053869
HIF1alpha_2x_Up	0.022692274	0.0719027
Myeloma_TACI_high_bone_marrow_plasma_cell_gene	0.007082114	0.07819874
IRF4_myeloma_induced_all	0.042573559	0.0789714
Quiescence_heme_cluster1	0.169138112	0.07997643
STAT3_up_OCILy10	0.001262827	0.08033321
GMP_down_Ebert_cell_11	0.054487672	0.08388987
Tcell_cytokine_induced_IL2_IL7_IL15only	0.096109442	0.08697712

ARID1A_mut_up_141_Ash_FL	0.000225466	0.09098391
Bcell_up_Ebert_cell_11	0.008427595	0.09766132
CREBBP_mut_down_278_Ash_FL	2.05E-05	0.09829637
ABC_gt_GCB_LC	0.072357188	0.10031351
IKZF1_CB_prom	0.004076355	0.12075224
Myeloma_CD-1_subgroup_down	0.028846856	0.12831562
CLL_unmutated_gt_CLL_mutated	0.058332071	0.12963861
IL6_Ly10_Up_group1	0.02450311	0.13813767
Tcell_cytokine_induced_IL2_IL7_IL15_IL4	0.03212458	0.13813767
KLF2_induced	0.034662173	0.13813767
PAX5_repressed	0.022692274	0.13832894
Glutamine_starve_up	0.019180578	0.14659626
mouse_shCrebbp.r2.up_328	1.07E-06	0.147274
p53_targets	0.043226471	0.15732263
ERY_up_Ebert_cell_11	6.41E-08	0.16541145
Cell_cycle_Cho	0.072896804	0.17100362
Myeloma_CD-2_subgroup_down	0.00368102	0.17124751
Glucose_starve_up	0.032524053	0.17869434
IL6_Ly10_Up_group2	0.019209857	0.18170586
mouse.shCrebbp.r2.up_p.500	0.033608563	0.18331803
Reticulocyte_large	0.03212458	0.18981108
Ly1_siBCL6_48h_upreg	0.003926958	0.19647044
Ribosomal_protein	0.001323949	0.20227331
Regulatory_T_cell_McHugh_Herman_concensus	0.006610756	0.20227331
XBP1_target_other	0.007166255	0.20227331
KLF2_repressed	0.01066673	0.20227331
mouse.shCrebbp.r2.0_p.1000_up	0.0002737	0.21446663
EZH2_mut_down_347_Ash_FL	0.016484676	0.22045291
Myc_RNAi_OCILy3	0.000429148	0.22416597
Myc_overexpression_2x_up	0.004411547	0.24104483
EP300_mut_down_271_Ash_FL	1.16E-07	0.25199026
Quiescence_heme_cluster3	0.054352349	0.25199026
HSC_up_Ebert_cell_11	1.34E-06	0.25208322
CNS_Node1661	0.040434507	0.25208322
STAT3high_ABC_DLBCL_subgroup	0.09220422	0.26742765
KMT2C_mut_down_214_Ash_FL	0.035309108	0.30271318
Notch_T-ALL_down_Palomero	0.091825369	0.30271318
BCL6_targets_CHIPCHIP	0.03566405	0.30763561
ly1.enhancer.DISTAL.BCL6-SMRT.DRE.553	0.031149094	0.31540009
Erythroid_precursor_GNF	0.004993067	0.31786876
ly1.promoter.BCL6.SMRT.BCOR.341	0.006610756	0.31911011
Tcell_cytokine_induced_prolif	0.042567694	0.33421866
GCB.promoter.BCL6.alone.106	0.096917969	0.3736361
c2.Crebbp.up_205	0.097621462	0.3736361
c2.Crebbp.up_500	0.097621462	0.3736361
BCL6_repressed	0.004665623	0.3847894
Resting_dendritic_cell_GNF	0.074249037	0.39729193
Myeloma_TACI_low_plasmablast_gene	0.081705409	0.40226843
c2.Ep300.down_468	0.086441999	0.40978062
c1.Crebbp.up_198	0.096109442	0.44857895
Serum_response_Fb_down	0.001739318	0.46848795
Promoter_loss.ATAC.reads_CREBBP.KD	0.094827934	0.46848795
Cell_cycle_Whitfield	0.038650906	0.51285705

PGC-1alpha_overepxression_up	0.001074677	0.54932556
Myc_overexpression_1.5x_up	0.003375371	NA
Notch_T-ALL_up_Palomero	0.019037179	NA
HIF1alpha_1.5x_down	0.02659487	NA
KMT2D_mut_up_20_Ash_FL	0.081705409	NA

Supplementary Table 9. Number and percentage of clones with at least one C-to-T mutation among clones identified in GC B-cells.

Sample	Total number of clones identified	Number of clones with at least one C-to-T mutation at WRC motif	Percentage of clones with at least one C-to-T mutation among all identified clones
TET2 wild-type 1	35830	4426	12.3528
TET2 wild-type 2	40537	4682	11.5499
TET2 wild-type 3	36934	4190	11.3446
TET2 deficient 1	47622	5263	11.0516
TET2 deficient 2	35030	3984	11.3731

Supplementary Table 10. Mouse and human pathways enriched by hypermethylated genes.

Species	pathway	log2FC	p-value	FDR
Mouse	c3.Crebbp.down 500	1.6275	2.89E-07	6.57E-05
Mouse	P300 ly1 enhancer	0.7084	3.88E-05	0.0044072
Mouse	Pan B U133plus	1.9573	0.000207	0.01563117
Mouse	Blimp Bcell repressed	2.1208	0.000399	0.02262265
Mouse	B cell down anergy	3.7058	0.000903	0.03589764
Mouse	Resting blood B cell GNF	1.8053	0.000949	0.03589764
Mouse	Ly1 BCL6RD2mut upreg	0.4588	0.00217	0.05908272
Mouse	mouse.shCrebbp.r2.down p.500	1.0396	0.002342	0.05908272
Mouse	LZvsDZ Teater CC Up vs CB	0.8535	0.001852	0.05908272
Mouse	Myc ChIP PET 2plus	0.2917	0.002974	0.0613769
Mouse	GO BP MM ANTIGEN PROCESSING AND PRESENTATION OF EXOGENOUS PEPTIDE ANTIGEN VIA MHC CLASS II	3.2203	0.002948	0.0613769
Mouse	GCB bivalent Prom genes	0.3791	0.003761	0.07113932
Mouse	denovobivGenes	0.5321	0.004649	0.08118707
Mouse	KLF2 induced	1.2439	0.006635	0.08704311
Mouse	ly1.promoter.BCL6-SMRT.all.451	0.7259	0.007286	0.08704311
Mouse	mouse shCrebbp.r2.down 545	0.7588	0.005421	0.08704311
Mouse	mouse.shCrebbp.r2.0 p.1000 down	0.7148	0.007035	0.08704311
Mouse	c1.Crebbp.down 500	0.8463	0.006879	0.08704311
Mouse	KEGG ANTIGEN PROCESSING AND PRESENTATION	1.6651	0.006	0.08704311
Mouse	CD40 upregulated Burkitt lymphoma	1.3459	0.0086	0.09778529
Human	EZH2_target_ChIP	1.6531	1.26E-26	1.68E-24
Human	GCB_bivalentProm_genes	1.3105	6.22E-15	4.17E-13
Human	CNS_PNS_Node1663	1.7255	9.45E-06	0.00042195
Human	CTCF_CB_all	0.2726	1.96E-05	0.00065695
Human	Ly1_BCL6RD2mut_upreg	0.8671	5.52E-05	0.00147992
Human	CTCF_CB_enhancer	0.2976	0.000122	0.00233509
Human	c1.Crebbp.up_198	2.1034	0.000114	0.00233509
Human	CTCF_ly1_enhancer	0.1964	0.00016	0.0026871
Human	CTCF_CB_prom	0.6047	0.000303	0.00451599
Human	E2F3_overexpression_4x_up	2.7381	0.000848	0.01127455
Human	Resting_monocyte_GNF	1.8453	0.000926	0.01127455
Human	CTCF_NB_all	0.2209	0.001397	0.01560155
Human	CTCF_NB_enhancer	0.2635	0.001633	0.01562713
Human	CTCF_ly1_all	0.1249	0.001542	0.01562713

Human	E2F3_overexpression_2x_up	1.7572	0.002592	0.02315555
Human	denovobivGenes	0.8135	0.003175	0.02659127
Human	Enhancer_loss.ATAC.reads_CREBBP.KD	0.8899	0.004083	0.03218432
Human	SREBP1a&2_up_Scap_indep	3.0791	0.004972	0.03701668
Human	Myeloma_TACI_high_bone_marrow_plasma_cell_gene	1.8567	0.006275	0.04425301
Human	c2.Ep300.down_468	1.0748	0.007151	0.04791461
Human	Distal_loss.ATAC.reads_CREBBP.KD	1.0202	0.00764	0.04874729
Human	NB_GCB_Progression_All_Genes_RPKM_minus2.to.plus2	0.3076	0.009675	0.05892931
Human	GC_termDiff_Genes	0.5730	0.01147	0.06682486
Human	Bcell_down_Ebert_cell_11	1.1179	0.013225	0.07384086
Human	Resting_dendritic_cell_GNF	1.7381	0.017063	0.09145995
Human	mouse.shCrebbp.r2.down_p.500	1.1829	0.01839	0.09477701
Human	GC_T_helper_up4x_Chtanova	1.3319	0.021761	0.09705152
Human	GC_T_helper_up_Kim	1.9092	0.021657	0.09705152
Human	Lung_Node3969	3.0791	0.022452	0.09705152
Human	Ly1_siBCL6_48h_upreg	0.5635	0.022354	0.09705152
Human	Distal_gain.ATAC.reads_CREBBP.KD	1.4942	0.02004	0.09705152

REFERENCES AND NOTES

1. D. Hu, A. Shilatifard, Epigenetics of hematopoiesis and hematological malignancies. *Genes Dev.* **30**, 2021–2041 (2016).

2. C. Mlynarczyk, L. Fontán, A. Melnick, Germinal center-derived lymphomas: The darkest side of humoral immunity. *Immunol. Rev.* **288**, 214–239 (2019).

3. Y. Jiang, P. M. Dominguez, A. M. Melnick, The many layers of epigenetic dysfunction in B-cell lymphomas. *Curr. Opin. Hematol.* **23**, 377–384 (2016).

4. A. Alhejaily, A. G. Day, H. E. Feilotter, T. Baetz, D. P. Lebrun, Inactivation of the *CDKN2A* tumor-suppressor gene by deletion or methylation is common at diagnosis in follicular lymphoma and associated with poor clinical outcome. *Clin. Cancer Res.* **20**, 1676–1686 (2014).

5. N. Chambwe, M. Kormaksson, H. Geng, S. De, F. Michor, N. A. Johnson, R. D. Morin, D. W. Scott, L. A. Godley, R. D. Gascoyne, A. Melnick, F. Campagne, R. Shaknovich, Variability in DNA methylation defines novel epigenetic subgroups of DLBCL associated with different clinical outcomes. *Blood* **123**, 1699–1708 (2014).

6. S. De, R. Shaknovich, M. Riester, O. Elemento, H. Geng, M. Kormaksson, Y. Jiang, B. Woolcock, N. Johnson, J. M. Polo, L. Cerchietti, R. D. Gascoyne, A. Melnick, F. Michor, Aberration in DNA methylation in B-cell lymphomas has a complex origin and increases with disease severity. *PLOS Genet.* **9**, e1003137 (2013).

7. T. Clozel, S. Yang, R. L. Elstrom, W. Tam, P. Martin, M. Kormaksson, S. Banerjee, A. Vasanthakumar, B. Culjkovic, D. W. Scott, S. Wyman, M. Leser, R. Shaknovich, A. Chadburn, F. Tabbo, L. A. Godley, R. D. Gascoyne, K. L. Borden, G. Inghirami, J. P. Leonard, A. Melnick, L. Cerchietti, Mechanism-based epigenetic chemosensitization therapy of diffuse large B-cell lymphoma. *Cancer Discov.* **3**, 1002–1019 (2013).

8. A. M. Deaton, A. Bird, CpG islands and the regulation of transcription. *Genes Dev.* **25**, 1010–1022 (2011).

9. X. Wu, Y. Zhang, TET-mediated active DNA demethylation: Mechanism, function and beyond. *Nat. Rev. Genet.* **18**, 517–534 (2017).

10. R. Rampal, A. Alkalin, J. Madzo, A. Vasanthakumar, E. Pronier, J. Patel, Y. Li, J. Ahn, O. Abdel-Wahab, A. Shih, C. Lu, P. S. Ward, J. J. Tsai, T. Hricik, V. Tosello, J. E. Tallman, X. Zhao, D. Daniels, Q. Dai, L. Ciminio, I. Aifantis, C. He, F. Fuks, M. S. Tallman, A. Ferrando, S. Nimer, E. Paietta, C. B. Thompson, J. D. Licht, C. E. Mason, L. A. Godley, A. Melnick, M. E. Figueroa, R. L. Levine, DNA hydroxymethylation profiling reveals that *WT1* mutations result in loss of TET2 function in acute myeloid leukemia. *Cell Rep.* **9**, 1841–1855 (2014).

11. G. C. Hon, C.-X. Song, T. du, F. Jin, S. Selvaraj, A. Y. Lee, C. A. Yen, Z. Ye, S.-Q. Mao, B.-A. Wang, S. Kuan, L. E. Edsall, B. S. Zhao, G.-L. Xu, C. He, B. Ren, 5mC oxidation by Tet2 modulates enhancer activity and timing of transcriptome reprogramming during differentiation. *Mol. Cell* **56**, 286–297 (2014).

12. F. Asmar, V. Punj, J. Christensen, M. T. Pedersen, A. Pedersen, A. B. Nielsen, C. Hother, U. Ralfkiaer, P. Brown, E. Ralfkiaer, K. Helin, K. Grønbæk, Genome-wide profiling identifies a DNA methylation signature that associates with *TET2* mutations in diffuse large B-cell lymphoma. *Haematologica* **98**, 1912–1920 (2013).

13. A. Reddy, J. Zhang, N. S. Davis, A. B. Moffitt, C. L. Love, A. Waldrop, S. Leppa, A. Pasanen, L. Meriranta, M. L. Karjalainen-Lindsberg, P. Nørgaard, M. Pedersen, A. O. Gang, E. Høgdall, T. B. Heavican, W. Lone, J. Iqbal, Q. Qin, G. Li, S. Y. Kim, J. Healy, K. L. Richards, Y. Fedoriw, L. Bernal-Mizrachi, J. L. Koff, A. D. Staton, C. R. Flowers, O. Paltiel, N. Goldschmidt, M. Calaminici, A. Clear, J. Gribben, E. Nguyen, M. B. Czader, S. L. Ondrejka, A. Collie, E. D. Hsi, E. Tse, R. K. H. Au-Yeung, Y.-L. Kwong, G. Srivastava, W. W. L. Choi, A. M. Evens, M. Pilichowska, M. Sengar, N. Reddy, S. Li, A. Chadburn, L. I. Gordon, E. S. Jaffe, S. Levy, R. Rempel, T. Tzeng, L. E. Happ, T. Dave, D. Rajagopalan, J. Datta, D. B. Dunson, S. S. Dave, Genetic and functional drivers of diffuse large B cell lymphoma. *Cell* **171**, 481–494.e15 (2017).

14. P. M. Dominguez, H. Ghamlouch, W. Rosikiewicz, P. Kumar, W. Béguelin, L. Fontán, M. A. Rivas, P. Pawlikowska, M. Armand, E. Mouly, M. Torres-Martin, A. S. Doane, M. T. Calvo Fernandez, M. Durant, V. Della-Valle, M. Teater, L. Cimmino, N. Droin, S. Tadros, S. Motanagh, A. H. Shih, M.

A. Rubin, W. Tam, I. Aifantis, R. L. Levine, O. Elemento, G. Inghirami, M. R. Green, M. E. Figueroa, O. A. Bernard, S. Aoufouchi, S. Li, R. Shaknovich, A. M. Melnick, TET2 deficiency causes germinal center hyperplasia, impairs plasma cell differentiation, and promotes B-cell lymphomagenesis. *Cancer Discov.* **8**, 1632–1653 (2018).

15. C. Quivoron, L. Couronné, V. Della Valle, C. K. Lopez, I. Plo, O. Wagner-Ballon, M. Do Cruzeiro, F. Delhommeau, B. Arnulf, M.-H. Stern, L. Godley, P. Opolon, H. Tilly, E. Solary, Y. Duffourd, P. Dessen, H. Merle-Beral, F. Nguyen-Khac, M. Fontenay, W. Vainchenker, C. Bastard, T. Mercher, O. A. Bernard, TET2 inactivation results in pleiotropic hematopoietic abnormalities in mouse and is a recurrent event during human lymphomagenesis. *Cancer Cell* **20**, 25–38 (2011).

16. F. Delhommeau, S. Dupont, V. D. Valle, C. James, S. Trannoy, A. Massé, O. Kosmider, J.-P. Le Couedic, F. Robert, A. Alberdi, Y. Lécluse, I. Plo, F. J. Dreyfus, C. Marzac, N. Casadevall, C. Lacombe, S. P. Romana, P. Dessen, J. Soulier, F. Viguié, M. Fontenay, W. Vainchenker, O. A. Bernard, Mutation in TET2 in myeloid cancers. *N. Engl. J. Med.* **360**, 2289–2301 (2009).

17. F. Lemonnier, L. Couronné, M. Parrens, J.-P. Jaïs, M. Travert, L. Lamant, O. Tournillac, T. Rousset, B. Fabiani, R. A. Cairns, T. Mak, C. Bastard, O. A. Bernard, L. de Leval, P. Gaulard, Recurrent TET2 mutations in peripheral T-cell lymphomas correlate with TFH-like features and adverse clinical parameters. *Blood* **120**, 1466–1469 (2012).

18. M. M. Patnaik, M. F. Zahid, T. L. Lasho, C. Finke, R. L. Ketterling, N. Gangat, K. D. Robertson, C. A. Hanson, A. Tefferi, Number and type of TET2 mutations in chronic myelomonocytic leukemia and their clinical relevance. *Blood Cancer J.* **6**, e472 (2016).

19. C.-W. J. Lio, V. Shukla, D. Samaniego-Castruita, E. González-Avalos, A. Chakraborty, X. Yue, D. G. Schatz, F. Ay, A. Rao, TET enzymes augment activation-induced deaminase (AID) expression via 5-hydroxymethylcytosine modifications at the *Aicda* superenhancer. *Sci. Immunol.* **4**, eaau7523 (2019).

20. E. Mouly, H. Ghamlouch, V. Della-Valle, L. Scourzic, C. Quivoron, D. Roos-Weil, P. Pawlikowska, V. Saada, M. K. Diop, C. K. Lopez, M. Fontenay, P. Dessen, I. P. Touw, T. Mercher, S. Aoufouchi, O. A. Bernard, B-cell tumor development in *Tet2*-deficient mice. *Blood Adv.* **2**, 703–714 (2018).

21. P. M. Dominguez, M. Teater, N. Chambwe, M. Kormaksson, D. Redmond, J. Ishii, B. Vuong, J. Chaudhuri, A. Melnick, A. Vasanthakumar, L. A. Godley, F. N. Papavasiliou, O. Elemento, R. Shaknovich, DNA methylation dynamics of germinal center B cells are mediated by AID. *Cell Rep.* **12**, 2086–2098 (2015).

22. R. Shaknovich, L. Cerchietti, L. Tsikitas, M. Kormaksson, S. de, M. E. Figueroa, G. Ballon, S. N. Yang, N. Weinhold, M. Reimers, T. Clozel, K. Luttrop, T. J. Ekstrom, J. Frank, A. Vasanthakumar, L. A. Godley, F. Michor, O. Elemento, A. Melnick, DNA methyltransferase 1 and DNA methylation patterning contribute to germinal center B-cell differentiation. *Blood* **118**, 3559–3569 (2011).

23. L. Wang, P. A. Ozark, E. R. Smith, Z. Zhao, S. A. Marshall, E. J. Rendleman, A. Piunti, C. Ryan, A. L. Whelan, K. A. Helmin, M. A. Morgan, L. Zou, B. D. Singer, A. Shilatifard, TET2 coactivates gene expression through demethylation of enhancers. *Sci. Adv.* **4**, eaau6986 (2018).

24. A. Lex, N. Gehlenborg, H. Strobelt, R. Vuillemot, H. Pfister, UpSet: Visualization of intersecting sets. *IEEE Trans. Vis. Comput. Graph.* **20**, 1983–1992 (2014).

25. Y. Jiang, A. Ortega-Molina, H. Geng, H.-Y. Ying, K. Hatzi, S. Parsa, D. McNally, L. Wang, A. S. Doane, X. Agirre, M. Teater, C. Meydan, Z. Li, D. Poloway, S. Wang, D. Ennishi, D. W. Scott, K. R. Stengel, J. E. Kranz, E. Holson, S. Sharma, J. W. Young, C.-S. Chu, R. G. Roeder, R. Shaknovich, S. W. Hiebert, R. D. Gascoyne, W. Tam, O. Elemento, H.-G. Wendel, A. M. Melnick, *CREBBP* inactivation promotes the development of HDAC3-dependent lymphomas. *Cancer Discov.* **7**, 38–53 (2017).

26. W. Béguelin, R. Popovic, M. Teater, Y. Jiang, K. L. Bunting, M. Rosen, H. Shen, S. N. Yang, L. Wang, T. Ezponda, E. Martinez-Garcia, H. Zhang, Y. Zheng, S. K. Verma, M. T. Mc Cabe, H. M. Ott, G. S. Van Aller, R. G. Kruger, Y. Liu, C. F. McHugh, D. W. Scott, Y. R. Chung, N. Kelleher, R. Shaknovich, C. L. Creasy, R. D. Gascoyne, K.-K. Wong, L. Cerchietti, R. L. Levine, O. Abdel-Wahab, J. D. Licht, O. Elemento, A. M. Melnick, EZH2 is required for germinal center formation and somatic EZH2 mutations promote lymphoid transformation. *Cancer Cell* **23**, 677–692 (2013).

27. S. Li, K. M. Paulsson, S. Chen, H. O. Sjögren, P. Wang, Tapasin is required for efficient peptide binding to transporter associated with antigen processing. *J. Biol. Chem.* **275**, 1581–1586 (2000).

28. B. Park, K. Ahn, An essential function of tapasin in quality control of HLA-G molecules. *J. Biol. Chem.* **278**, 14337–14345 (2003).

29. C.-W. J. Lio, V. Shukla, D. Samaniego-Castruita, E. González-Avalos, A. Chakraborty, X. Yue, D. G. Schatz, F. Ay, A. Rao, TET enzymes augment AID expression via 5hmC modifications at the Aicda superenhancer. *bioRxiv*, 438531 (2018).

30. H. W. Mittrücker, T. Matsuyama, A. Grossman, T. M. Kündig, J. Potter, A. Shahinian, A. Wakeham, B. Patterson, P. S. Ohashi, T. W. Mak, Requirement for the transcription factor LSIRF/IRF4 for mature B and T lymphocyte function. *Science* **275**, 540–543 (1997).

31. R. Kennedy, U. Klein, Aberrant activation of NF-κB signalling in aggressive lymphoid malignancies. *Cell* **7**, 189 (2018).

32. C.-W. Lio, J. Zhang, E. González-Avalos, P. G. Hogan, X. Chang, A. Rao, Tet2 and Tet3 cooperate with B-lineage transcription factors to regulate DNA modification and chromatin accessibility. *eLife* **5**, e18290 (2016).

33. Y. Yin, E. Morgunova, A. Jolma, E. Kaasinen, B. Sahu, S. Khund-Sayeed, P. K. Das, T. Kivioja, K. Dave, F. Zhong, K. R. Nitta, M. Taipale, A. Popov, P. A. Ginno, S. Domcke, J. Yan, D. Schübeler, C. Vinson, J. Taipale, Impact of cytosine methylation on DNA binding specificities of human transcription factors. *Science* **356**, eaaj2239 (2017).

34. Q. X. Xuan Lin, S. Sian, O. An, D. Thieffry, S. Jha, T. Benoukraf, MethMotif: An integrative cell specific database of transcription factor binding motifs coupled with DNA methylation profiles. *Nucleic Acids Res.* **47**, D145-D154 (2019).

35. G. Wang, X. Luo, J. Wang, J. Wan, S. Xia, H. Zhu, J. Qian, Y. Wang, MeDReaders: A database for transcription factors that bind to methylated DNA. *Nucleic Acids Res.* **46**, D146-D151 (2018).

36. Y. Jiang, T. D. Soong, L. Wang, A. M. Melnick, O. Elemento, Genome-wide detection of genes targeted by non-Ig somatic hypermutation in lymphoma. *PLOS ONE* **7**, e40332 (2012).

37. S. Cortellino, J. Xu, M. Sannai, R. Moore, E. Caretti, A. Cigliano, M. le Coz, K. Devarajan, A. Wessels, D. Soprano, L. K. Abramowitz, M. S. Bartolomei, F. Rambow, M. R. Bassi, T. Bruno, M. Fanciulli, C. Renner, A. J. Klein-Szanto, Y. Matsumoto, D. Kobi, I. Davidson, C. Alberti, L. Larue, A. Bellacosa, Thymine DNA glycosylase is essential for active DNA demethylation by linked deamination-base excision repair. *Cell* **146**, 67–79 (2011).

38. J. U. Guo, Y. Su, C. Zhong, G.-L. Ming, H. Song, Hydroxylation of 5-methylcytosine by TET1 promotes active DNA demethylation in the adult brain. *Cell* **145**, 423–434 (2011).

39. S. Kumar, V. Chinnusamy, T. Mohapatra, Epigenetics of modified DNA bases: 5-methylcytosine and beyond. *Front. Genet.* **9**, 640 (2018).

40. T. Pfaffeneder, F. Spada, M. Wagner, C. Brandmayr, S. K. Laube, D. Eisen, M. Truss, J. Steinbacher, B. Hackner, O. Kotljarova, D. Schuermann, S. Michalakis, O. Kosmatchev, S. Schiesser, B. Steigenberger, N. Raddaoui, G. Kashiwazaki, U. Müller, C. G. Spruijt, M. Vermeulen, H. Leonhardt, P. Schär, M. Müller, T. Carell, Tet oxidizes thymine to 5-hydroxymethyluracil in mouse embryonic stem cell DNA. *Nat. Chem. Biol.* **10**, 574–581 (2014).

41. M. Muramatsu, V. S. Sankaranand, S. Anant, M. Sugai, K. Kinoshita, N. O. Davidson, T. Honjo, Specific expression of activation-induced cytidine deaminase (AID), a novel member of the RNA-editing deaminase family in germinal center B cells. *J. Biol. Chem.* **274**, 18470–18476 (1999).

42. B. Reina-San-Martin, S. Difilippantonio, L. Hanitsch, R. F. Masilamani, A. Nussenzweig, M. C. Nussenzweig, H2AX is required for recombination between immunoglobulin switch regions but not for intra-switch region recombination or somatic hypermutation. *J. Exp. Med.* **197**, 1767–1778 (2003).

43. S. Zheng, B. Q. Vuong, B. Vaidyanathan, J.-Y. Lin, F.-T. Huang, J. Chaudhuri, Non-coding RNA Generated following Lariat debranching mediates targeting of AID to DNA. *Cell* **161**, 762–773 (2015).

44. P. Pham, R. Bransteitter, J. Petruska, M. F. Goodman, Processive AID-catalysed cytosine deamination on single-stranded DNA simulates somatic hypermutation. *Nature* **424**, 103–107 (2003).

45. K. D. Rasmussen, K. Helin, Role of TET enzymes in DNA methylation, development, and cancer. *Genes Dev.* **30**, 733–750 (2016).

46. D. Zotos, J. M. Coquet, Y. Zhang, A. Light, K. D'Costa, A. Kallies, L. M. Corcoran, D. I. Godfrey, K.-M. Toellner, M. J. Smyth, S. L. Nutt, D. M. Tarlinton, IL-21 regulates germinal center B cell differentiation and proliferation through a B cell-intrinsic mechanism. *J. Exp. Med.* **207**, 365–378 (2010).

47. A. Turqueti-Neves, M. Otte, O. P. da Costa, U. E. Höpken, M. Lipp, T. Buch, D. Voehringer, B-cell-intrinsic STAT6 signaling controls germinal center formation. *Eur. J. Immunol.* **44**, 2130–2138 (2014).

48. J. J. Jeong, X. Gu, J. Nie, S. Sundaravel, H. Liu, W.-L. Kuo, T. D. Bhagat, K. Pradhan, J. Cao, S. Nischal, K. L. McGraw, S. Bhattacharyya, M. R. Bishop, A. Artz, M. J. Thirman, A. Moliterno, P. Ji, R. L. Levine, L. A. Godley, U. Steidl, J. J. Bieker, A. F. List, Y. Saunthararajah, C. He, A. Verma, A. Wickrema, Cytokine-regulated phosphorylation and activation of TET2 by JAK2 in hematopoiesis. *Cancer Discov.* **9**, 778–795 (2019).

49. P. M. Dominguez, M. Teater, R. Shaknovich, The new frontier of epigenetic heterogeneity in B-cell neoplasms. *Curr. Opin. Hematol.* **24**, 402–408 (2017).

50. C. S. Nabel, H. Jia, Y. Ye, L. Shen, H. L. Goldschmidt, J. T. Stivers, Y. Zhang, R. M. Kohli, AID/APOBEC deaminases disfavor modified cytosines implicated in DNA demethylation. *Nat. Chem. Biol.* **8**, 751–758 (2012).

51. G. Rangam, K.-M. Schmitz, A. J. A. Cobb, S. K. Petersen-Mahrt, AID enzymatic activity is inversely proportional to the size of cytosine C5 orbital cloud. *PLOS ONE* **7**, e43279 (2012).

52. P. M. Dominguez, R. Shaknovich, Epigenetic function of activation-induced cytidine deaminase and its link to lymphomagenesis. *Front. Immunol.* **5**, 642 (2014).

53. C. Duy, M. Teater, F. E. Garrett-Bakelman, T. C. Lee, C. Meydan, J. L. Glass, M. Li, J. C. Hellmuth, H. P. Mohammad, K. N. Smitheman, A. H. Shih, O. Abdel-Wahab, M. S. Tallman, M. L. Guzman, D. Muench, H. L. Grimes, G. J. Roboz, R. G. Kruger, C. L. Creasy, E. M. Paietta, R. L. Levine, M. Carroll, A. M. Melnick, Rational targeting of cooperating layers of the epigenome yields enhanced therapeutic efficacy against AML. *Cancer Discov.* **9**, 872–889 (2019).

54. K. Moran-Crusio, L. Reavie, A. Shih, O. Abdel-Wahab, D. Ndiaye-Lobry, C. Lobry, M. E. Figueroa, A. Vasanthakumar, J. Patel, X. Zhao, F. Perna, S. Pandey, J. Madzo, C. Song, Q. Dai, C. He, S. Ibrahim, M. Beran, J. Zavadil, S. D. Nimer, A. Melnick, L. A. Godley, I. Aifantis, R. L. Levine, *Tet2* loss leads to increased hematopoietic stem cell self-renewal and myeloid transformation. *Cancer Cell* **20**, 11–24 (2011).

55. I. García-Ramírez, S. Tadros, I. González-Herrero, A. Martín-Lorenzo, G. Rodríguez-Hernández, D. Moore, L. Ruiz-Roca, O. Blanco, D. Alonso-López, J. D. L. Rivas, K. Hartert, R. Duval, D. Klinkebiel, M. Bast, J. Vose, M. Lunning, K. Fu, T. Greiner, F. Rodrigues-Lima, R. Jiménez, F. J. G. Criado, Ma. B. G. Cenador, P. Brindle, C. Vicente-Dueñas, A. Alizadeh, I. Sánchez-García, M. R. Green, *Crebbp* loss cooperates with *Bcl2* overexpression to promote lymphoma in mice. *Blood* **129**, 2645–2656 (2017).

56. G. Lenz, G. Wright, S. S. Dave, W. Xiao, J. Powell, H. Zhao, W. Xu, B. Tan, N. Goldschmidt, J. Iqbal, J. Vose, M. Bast, K. Fu, D. D. Weisenburger, T. C. Greiner, J. O. Armitage, A. Kyle, L. May, R. D. Gascoyne, J. M. Connors, G. Troen, H. Holte, S. Kvaloy, D. Dierickx, G. Verhoef, J. Delabie, E. B. Smeland, P. Jares, A. Martinez, A. Lopez-Guillermo, E. Montserrat, E. Campo, R. M. Braziel, T. P. Miller, L. M. Rimsza, J. R. Cook, B. Pohlman, J. Sweetenham, R. R. Tubbs, R. I. Fisher, E. Hartmann, A. Rosenwald, G. Ott, H.-K. Muller-Hermelink, D. Wrench, T. A. Lister, E. S. Jaffe, W. H. Wilson, W. C. Chan, L. M. Staudt, Lymphoma/Leukemia Molecular Profiling Project, Stromal gene signatures in large-B-cell lymphomas. *N. Engl. J. Med.* **359**, 2313–2323 (2008).

57. A. Akalin, F. E. Garrett-Bakelman, M. Kormaksson, J. Busuttil, L. Zhang, I. Khrebtukova, T. A. Milne, Y. Huang, D. Biswas, J. L. Hess, C. D. Allis, R. G. Roeder, P. J. M. Valk, B. Löwenberg, R. Delwel, H. F. Fernandez, E. Paietta, M. S. Tallman, G. P. Schroth, C. E. Mason, A. Melnick, M. E.

Figueroa, Base-pair resolution DNA methylation sequencing reveals profoundly divergent epigenetic landscapes in acute myeloid leukemia. *PLOS Genet.* **8**, e1002781 (2012).

58. A. Akalin, M. Kormaksson, S. Li, F. E. Garrett-Bakelman, M. E. Figueroa, A. Melnick, C. E. Mason, methylKit: A comprehensive R package for the analysis of genome-wide DNA methylation profiles. *Genome Biol.* **13**, R87 (2012).

59. S. Heinz, C. Benner, N. Spann, E. Bertolino, Y. C. Lin, P. Laslo, J. X. Cheng, C. Murre, H. Singh, C. K. Glass, Simple combinations of lineage-determining transcription factors prime *cis*-regulatory elements required for macrophage and B cell identities. *Mol. Cell* **38**, 576–589 (2010).

60. A. Dobin, C. A. Davis, F. Schlesinger, J. Drenkow, C. Zaleski, S. Jha, P. Batut, M. Chaisson, T. R. Gingeras, STAR: Ultrafast universal RNA-seq aligner. *Bioinformatics* **29**, 15–21 (2013).

61. Y. Liao, G. K. Smyth, W. Shi, The Subread aligner: Fast, accurate and scalable read mapping by seed-and-vote. *Nucleic Acids Res.* **41**, e108 (2013).

62. N. Ignatiadis, B. Klaus, J. B. Zaugg, W. Huber, Data-driven hypothesis weighting increases detection power in genome-scale multiple testing. *Nat. Methods* **13**, 577–580 (2016).

63. M. I. Love, W. Huber, S. Anders, Moderated estimation of fold change and dispersion for RNA-seq data with DESeq2. *Genome Biol.* **15**, 550 (2014).

64. R. Bourgon, R. Gentleman, W. Huber, Independent filtering increases detection power for high-throughput experiments. *Proc. Natl. Acad. Sci. U.S.A.* **107**, 9546–9551 (2010).

65. M. E. Ritchie, B. Phipson, D. Wu, Y. Hu, C. W. Law, W. Shi, G. K. Smyth, *limma* powers differential expression analyses for RNA-sequencing and microarray studies. *Nucleic Acids Res.* **43**, e47 (2015).

66. M. Martin, Cutadapt removes adapter sequences from high-throughput sequencing reads. *EMBnet.journal* **17**, 10–12 (2011).

67. B. Langmead, S. L. Salzberg, Fast gapped-read alignment with bowtie 2. *Nat. Methods* **9**, 357–359 (2012).

68. Y. Zhang, T. Liu, C. A. Meyer, J. Eeckhoute, D. S. Johnson, B. E. Bernstein, C. Nussbaum, R. M. Myers, M. Brown, W. Li, X. S. Liu, Model-based analysis of ChIP-Seq (MACS). *Genome Biol.* **9**, R137 (2008).

69. V. K. Mootha, C. M. Lindgren, K.-F. Eriksson, A. Subramanian, S. Sihag, J. Lehar, P. Puigserver, E. Carlsson, M. Ridderstråle, E. Laurila, N. Houstis, M. J. Daly, N. Patterson, J. P. Mesirov, T. R. Golub, P. Tamayo, B. Spiegelman, E. S. Lander, J. N. Hirschhorn, D. Altshuler, L. C. Groop, PGC-1α-responsive genes involved in oxidative phosphorylation are coordinately downregulated in human diabetes. *Nat. Genet.* **34**, 267–273 (2003).

70. A. Subramanian, P. Tamayo, V. K. Mootha, S. Mukherjee, B. L. Ebert, M. A. Gillette, A. Paulovich, S. L. Pomeroy, T. R. Golub, E. S. Lander, J. P. Mesirov, Gene set enrichment analysis: A knowledge-based approach for interpreting genome-wide expression profiles. *Proc. Natl. Acad. Sci. U.S.A.* **102**, 15545–15550 (2005).

71. S. A. Armstrong, J. E. Staunton, L. B. Silverman, R. Pieters, M. L. den Boer, M. D. Minden, S. E. Sallan, E. S. Lander, T. R. Golub, S. J. Korsmeyer, MLL translocations specify a distinct gene expression profile that distinguishes a unique leukemia. *Nat. Genet.* **30**, 41–47 (2002).

72. A. Ortega-Molina, I. W. Boss, A. Canela, H. Pan, Y. Jiang, C. Zhao, M. Jiang, D. Hu, X. Agirre, I. Niesvizky, J.-E. Lee, H.-T. Chen, D. Ennishi, D. W. Scott, A. Mottok, C. Hother, S. Liu, X.-J. Cao, W. Tam, R. Shaknovich, B. A. Garcia, R. D. Gascoyne, K. Ge, A. Shilatifard, O. Elemento, A. Nussenzweig, A. M. Melnick, H.-G. Wendel, The histone lysine methyltransferase KMT2D sustains a gene expression program that represses B cell lymphoma development. *Nat. Med.* **21**, 1199–1208 (2015).

73. K. Hatzi, Y. Jiang, C. Huang, F. Garrett-Bakelman, M. D. Gearhart, E. G. Giannopoulou, P. Zumbo, K. Kirouac, S. Bhaskara, J. M. Polo, M. Kormaksson, A. D. MacKerell Jr., F. Xue, C. E. Mason, S. W. Hiebert, G. G. Prive, L. Cerchietti, V. J. Bardwell, O. Elemento, A. Melnick, A hybrid

mechanism of action for BCL6 in B cells defined by formation of functionally distinct complexes at enhancers and promoters. *Cell Rep.* **4**, 578–588 (2013).

74. S. Shaker, M. Bernstein, R. L. Momparler, Antineoplastic action of 5-aza-2′-deoxycytidine (Dacogen) and depsipeptide on Raji lymphoma cells. *Oncol. Rep.* **11**, 1253–1256 (2004).

75. L. Lai, J. Hennessey, V. Bares, E. W. Son, Y. Ban, W. Wang, J. Qi, G. Jiang, A. Liberzon, S. X. Ge, GSKB: A gene set database for pathway analysis in mouse. *bioRxiv.org*, 082511 (2016).

76. S. Aibar, C. B. González-Blas, T. Moerman, V. A. Huynh-Thu, H. Imrichova, G. Hulselmans, F. Rambow, J.-C. Marine, P. Geurts, J. Aerts, J. van den Oord, Z. K. Atak, J. Wouters, S. Aerts, SCENIC: Single-cell regulatory network inference and clustering. *Nat. Methods* **14**, 1083–1086 (2017).

77. C. J. Bult, J. A. Blake, C. L. Smith, J. A. Kadin, J. E. Richardson, Mouse Genome Database Group, *Nucleic Acids Res.* **47**, D801-D806 (2019).

78. H. Li, Aligning sequence reads, clone sequences and assembly contigs with BWA-MEM. arXiv:1303.3997, (2013).

79. A. Wilm, P. P. K. Aw, D. Bertrand, G. H. T. Yeo, S. H. Ong, C. H. Wong, C. C. Khor, R. Petric, M. L. Hibberd, N. Nagarajan, LoFreq: A sequence-quality aware, ultra-sensitive variant caller for uncovering cell-population heterogeneity from high-throughput sequencing datasets. *Nucleic Acids Res.* **40**, 11189–11201 (2012).

80. H. Li, A statistical framework for SNP calling, mutation discovery, association mapping and population genetical parameter estimation from sequencing data. *Bioinformatics* **27**, 2987–2993 (2011).

81. N. T. Gupta, J. A. Vander Heiden, M. Uduman, D. Gadala-Maria, G. Yaari, S. H. Kleinstein, Change-O: A toolkit for analyzing large-scale B cell immunoglobulin repertoire sequencing data. *Bioinformatics* **31**, 3356–3358 (2015).

82. J. A. Vander Heiden, G. Yaari, M. Uduman, J. N. H. Stern, K. C. O'Connor, D. A. Hafler, F. Vigneault, S. H. Kleinstein, pRESTO: A toolkit for processing high-throughput sequencing raw reads of lymphocyte receptor repertoires. *Bioinformatics* **30**, 1930–1932 (2014).